

Synthesis, Photophysical and Nonlinear Optical Properties of Macromolecular Architectures Featuring Octupolar Tris(bipyridine) Ruthenium(II) Moieties: Evidence for a Supramolecular Self-Ordering in a Dendritic Structure

Thomas Le Bouder,[†] Olivier Maury,[†] Arnaud Bondon,[†] Karine Costuas,[†] Edmond Amouyal,[§] Isabelle Ledoux,^{||} Joseph Zyss,^{||} and Hubert Le Bozec^{*,†}

Contribution from the Institut de Chimie de Rennes, UMR 6509 and 6511 CNRS-Université de Rennes 1, 35042 Rennes Cedex, France, Laboratoire de Chimie-Physique, UMR 8000 CNRS-Université de Paris Sud, 91405 Orsay, France, and Laboratoire de Photonique Quantique Moléculaire, Institut d'Alembert IFR 121, UMR 8537 CNRS-ENS Cachan, 61 avenue du Président Wilson, 94235 Cachan, France

Received May 16, 2003; E-mail: lebozec@univ-rennes1.fr

Abstract: The synthesis, photophysical and nonlinear optical properties of several new multi-octupolar tris(bipyridine) ruthenium complexes are reported. The preparation on these complexes is based on the initial construction of multipodal 4,4'-dialkylaminostyryl-2,2'-bipyridine ligands (DAAS-bpy). Thermally stable polyimides featuring octupolar ruthenium trisbipyridyl complexes have been readily obtained by a polycondensation reaction. The controlled coordination strategy of dipodal and tripodal bipyridines to ruthenium(II) has also been successfully used to build bimetallic, trimetallic as well as the first metallodendrimer made of seven metallo-octupoles. These polymetallic species exhibit very intense absorption bands in the visible and long-lived luminescence. The quadratic NLO-susceptibilities β of these macromolecules have been characterized by harmonic light scattering at 1.91 μm and compared with those of the corresponding monometallic species. The NLO studies clearly demonstrate a quasi-supramolecular ordering in the metallodendrimer.

Introduction

The acentric arrangement of chromophores in molecule-based materials for second-order nonlinear optics (NLO) is a critical challenge for device applications.¹ In this regard, several strategies have been intensively investigated, such as statistical orientation by electrical poling of NLO-polymers², predetermined orientation of NLO-phores by using the Langmuir–Blodgett technique³ or stepwise construction of multilayers.⁴ Typically, the NLO-phores used for such purposes, are dipolar molecules having the combination of large first-order hyper-

polarizability (β) and dipolar moment (μ) values. In addition, an excellent thermal and chemical stability is required for further use in optoelectronic devices. To overcome the problems associated with strong intermolecular interactions between such high $\mu\beta$ chromophores, a significant breakthrough was recently achieved by Dalton and co-workers who designed efficient poled NLO-polymers in which dipole/dipole interactions were minimized by spatial isolation of the NLO-phores either with a dendritic envelope⁵ or with the introduction of bulky substituents.⁶ An alternative elegant approach to acentric materials consists of the *pre-organization* of NLO active species within a multi-chromophoric dipolar system. Interesting results have been obtained with bis-chromophoric compounds^{7,8,9} and with the assembly of four dipoles in calix-[4]-arene derivatives.¹⁰

[†] Institut de Chimie de Rennes, UMR 6509 CNRS-Université de Rennes 1.

[‡] Institut de Chimie de Rennes, UMR 6511 CNRS-Université de Rennes 1.

[§] Laboratoire de Chimie-Physique, UMR 8000 CNRS-Université de Paris Sud.

^{||} Laboratoire de Photonique Quantique Moléculaire, UMR 8537 CNRS-ENS Cachan.

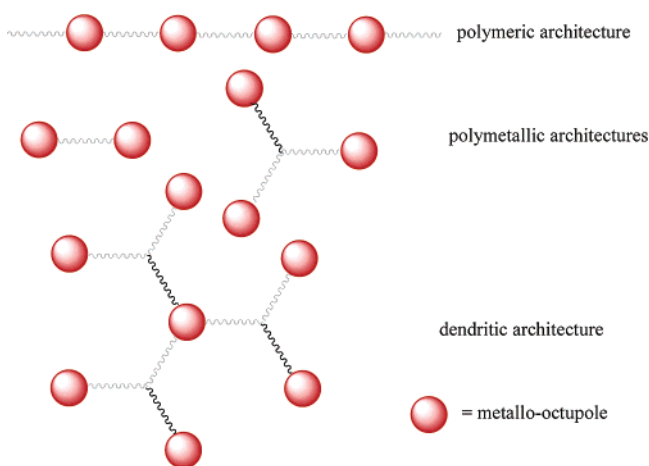
- (1) (a) Burland, D. M. *Chem. Rev.* (special issue) **1994**, *94*, 1–278. (b) *Molecular Nonlinear Optics: Materials, Physics and Devices*; Zyss, J., Ed.; Academic Press: Boston, 1994. (c) Marks, T. J.; Ratner, M. A. *Angew. Chem., Int. Ed. Engl.* **1995**, *34*, 155–173. (d) Dick, B.; Stegeman, R.; Twieg, R.; Zyss, J. *Chem. Phys.* (feature issue) **1999**, *245*, 1–568. (e) van der Boom, M. E. *Angew. Chem., Int. Ed. Engl.* **2002**, *41*, 3363–3366.
- (2) Burland, D. M.; Miller, R. D.; Walsh, C. A. *Chem. Rev.* **1994**, *94*, 31–75.
- (3) (a) Zang, K. Z.; Huang, C. H.; Xu, G. X.; Xu, Y.; Liu, Y. Q.; Zhu, D. B.; Zhao, X. S.; Xie, X. M.; Wu, N. Z. *Chem. Mater.* **1994**, *6*, 1986–1989. (b) Park, C. K.; Wijekoon, W. M. K. P.; Zhao, C.-F.; Prasad, P. N. *Chem. Mater.* **1994**, *6*, 1638–1641. (c) Baldwin, J. W.; Amareesh, R. R.; Peterson, I. R.; Shumate, W. J.; Cava, M. P.; Amiri, M. A.; Hamilton, R.; Ashwell, G. J.; Metzger, R. M. *J. Phys. Chem. B* **2002**, *106*, 12 158–12 164.

- (4) (a) Li, D. Q.; Ratner, M. A.; Marks, T. J.; Zhang, C. H.; Yang, J.; Wong, G. K. *J. Am. Chem. Soc.* **1990**, *112*, 7389–7390. (b) Katz, H. E.; Scheller, G.; Putvinski, T. M.; Schilling, M. L.; Wilson, W. L.; Chidsey, C. E. D. *Science* **1991**, *254*, 1485–1487. (c) Fachetti, A.; Abboto, A.; Beverina, L.; van der Boom, M. E.; Dutta, P.; Evmenenko, G.; Pagani, G. A.; Marks, T. J. *Chem. Mater.* **2003**, *15*, 1064–1072.
- (5) Ma, H.; Chen, B.; Sassa, T.; Dalton, L. R.; Jen, A. K.-Y. *J. Am. Chem. Soc.* **2001**, *123*, 986–987.
- (6) Shi, Y. Q.; Zhang, C.; Zang, H.; Bechtel, J. H.; Dalton, L. R.; Robinson, B. H.; Steier, W. H. *Science* **2000**, *288*, 119–122.
- (7) Fave, C.; Hissler, M.; Sénéchal, K.; Ledoux, I.; Zyss, J.; Réau, R. *Chem. Commun.* **2002**, 1674–1675.
- (8) (a) Deussen, H.-J.; Hendrickx, E.; Boutton, C.; Krogh, D.; Clays, K.; Bechgaard, K.; Persoons, A.; Bjørnholm, T. *J. Am. Chem. Soc.* **1996**, *118*, 6841–6852. (b) Deussen, H.-J.; Boutton, C.; Thorup, N.; Geisler, T.; Hendrickx, E.; Bechgaard, K.; Persoons, A.; Bjørnholm, T. *Chem. Eur. J.* **1998**, *4*, 240–250.

The pre-organization of a larger number of dipoles (from 7 up to 64) within supermolecules such as β -cyclodextrin¹¹ or dendrimers¹² has also recently been reported and opened the route to new noncentrosymmetric nano-objects combining very high molecular hyperpolarizability and huge dipole moment.

Nondipolar (Octupolar) materials would be able to overcome the problem of intermolecular dipole–dipole interactions.¹³ However, whereas octupolar nonlinearity has been largely demonstrated in molecular systems,¹⁴ its extension to supramolecular and macromolecular architectures remains a challenge.¹⁵ We have previously demonstrated that metal ions can act as powerful templates for the design of a variety of octupolar arrangements with large optical nonlinearities.¹⁶ Pursuing this work, we thought to use the wide possibilities offered by the supramolecular coordination chemistry¹⁷ to design multi-octu-

Chart 1



polar compounds such as polymetallic complexes, metallo-dendrimers or metallo-polymers.¹⁸

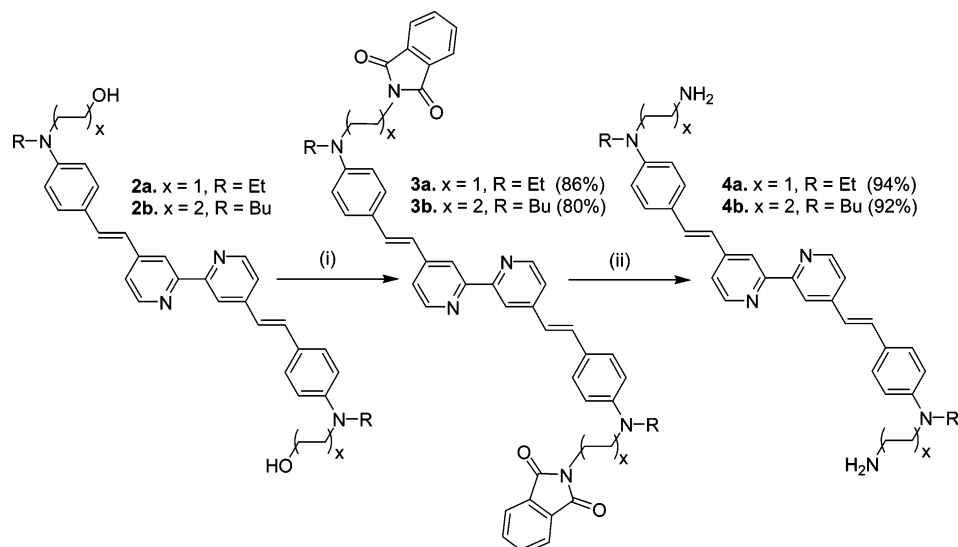
Among the variety of metallo-octupoles studied, tris(dialkylaminostyryl-[2,2']-bipyridine) zinc(II) or ruthenium(II) complexes exhibit the best tradeoff between NLO activity and thermal/chemical stability.¹⁹ Moreover, ruthenium(II) has the ability to form heteroleptic complexes upon sequential coordination of different bipyridyl ligands.²⁰ Therefore, for the design of multi-octupolar complexes, we sought to apply this concept which requires the initial construction of multipodal ligands based on dialkylaminostyryl-[2,2']-bipyridine (DAASbpy). In the present paper, we describe the synthesis and characterization of new polyimide, dipodal and tripodal ligands containing the DAASbpy moieties. These ligands are good building blocks for the construction of polymetallic octupolar architectures (dimer, trimer, heptamer and polymer, Chart 1).²¹ Their absorption, emission, and second-order nonlinear optical properties are discussed in details and compared with those of the corresponding monometallic species. The NLO studies performed at the near-IR 1.91 μm fundamental wavelength clearly demonstrates a quasi-supramolecular ordering in the dendrimer made of seven ruthenium(II) complexes.

Results and Discussion

I. Synthesis. (a) Main Chain Polyimides Containing Octupolar Ruthenium(II) NLO-Phores. The first part deals with the incorporation of tris(dialkylaminostyryl-[2,2']-bipyridyl) ruthenium(II) chromophores [alkyl = ethyl, *n*-butyl] into a polyimide backbone.²² Among the large variety of polymers designed for nonlinear optical purposes, polyimides have

- (9) For an brief introduction see: Nalwa, H. S.; Watanabe, T.; Miyata, S. *Adv. Mater.* **1995**, *7*, 754–758.
- (10) (a) Kenis, P. J. A.; Noordman, O. F. J.; Schönherr, H.; Kerver, E. G.; Snellink-Ruël, B. H. M.; van Hummel, G. J.; Harkema, S.; van der Vorst, C. P. J. M.; Hare, J.; Picken, S. J.; Enbersen, J. F. J.; van Hulst, N. F.; Vancsi, G. J.; Reinhoudt, D. N. *Chem. Eur. J.* **1998**, *4*, 1225–1234. (b) Kenis, P. J. A.; Kerver, E. G.; Snellink-Ruël, B. H. M.; van Hummel, G. J.; Harkema, S.; Flipse, M. C.; Woudenberg, R. H.; Enbersen, J. F. J.; Reinhoudt, D. N. *Eur. J. Org. Chem.* **1998**, 1089–1098. (c) Kenis, P. J. A.; Noordman, O. F. J.; Houbrechts, S.; van Hummel, G. J.; Harkema, S.; van Veggel, F. C. J. M.; Clays, K.; Enbersen, J. F. J.; Persoons, A.; van Hulst, N. F.; Vancsi, G. J.; Reinhoudt, D. N. *J. Am. Chem. Soc.* **1998**, *120*, 7875–7883.
- (11) Rekaï, E. D.; Baudin, J.-B.; Jullien, L.; Ledoux, I.; Zyss, J.; Blanchard-Desce, M. *Chem. Eur. J.* **2001**, *7*, 4395–4402.
- (12) (a) Put, E. J. H.; Clays, K.; Persoons, A.; Biemans, H. A. M.; Luijckx, C. P. M.; Meijer, E. W. *Chem. Phys. Lett.* **1996**, *260*, 136–141. (b) Yokoyama, S.; Nakahama, T.; Otomo, A.; Mashiko, S. *J. Am. Chem. Soc.* **2000**, *122*, 3174–3181. For other dipole-based dendritic structures whose NLO properties were not reported see: (c) Peng, Z.; Pan, Y.; Zhang, J. *J. Am. Chem. Soc.* **2000**, *122*, 6619–6623. (d) Wang, J.; Lu, M.; Pan, Y.; Peng, Z. *J. Org. Chem.* **2002**, *67*, 7881–7886. (e) Diez-Barra, E.; Garcia-Martinez, J. C.; Merino, S.; del Rey, R.; Rodriguez-Lopez, J.; Sanchez-Verdu, P.; Tejeda, J. *J. Org. Chem.* **2001**, *66*, 5664–5670.
- (13) (a) Zyss, J. *J. Chem. Phys.* **1993**, *98*, 6583–6599. (b) Zyss, J.; Ledoux, I. *Chem. Rev.* **1994**, *94*, 77–105.
- (14) For a review see: Ledoux, I.; Zyss, J. *C. R. Physique* **2002**, *3*, 407–427. For recent examples of octupolar structures see: (a) Wortmann, R.; Glania, C.; Krämer, P.; Matschiner, R.; Wolff, J. J.; Kraft, S.; Treptow, B.; Barbu, E.; Längle, D.; Görlitz, G. *Chem. Eur. J.* **1997**, *3*, 1765–1773. (b) Lambert, C.; Nöll, G.; Schmälzlin, E.; Meerholz, K.; Bräuchle, C. *Chem. Eur. J.* **1998**, *4*, 2129–2135. (c) Cho, B. R.; Lee, S. K.; Kim, K. A.; Son, K. N.; Kang, T. I.; Jeon, S. J. *Tetrahedron Lett.* **1998**, *39*, 9205–9208. (d) del Rey, B.; Keller, U.; Torres, T.; Rojo, G.; Agullo-Lopez, F.; Nonell, S.; Marti, C.; Brasselet, S.; Ledoux, I.; Zyss, J. *J. Am. Chem. Soc.* **1998**, *120*, 12 808–12 817. (e) Lambert, C.; Gaschler, W.; Schmälzlin, E.; Meerholz, K.; Bräuchle, C. *J. Chem. Soc., Perkin Trans.2* **1999**, 577–587. (f) Blanchard-Desce, M.; Baudin, J.-B.; Jullien, L.; Lorne, R.; Ruel, O.; Brasselet, S.; Zyss, J. *Optical Materials* **1999**, *12*, 333–338. (g) McDonagh, A. M.; Humphrey, M. G.; Samoc, M.; Luther-Davies, B.; Houbrechts, S.; Wada, T.; Sasabe, H.; Persoons, A. *J. Am. Chem. Soc.* **1999**, *121*, 1405–1406. (h) Andraud, C.; Zabalun, T.; Collet, A.; Zyss, J. *Chem. Phys.* **1999**, *245*, 243–261. (i) Bourgoigne, C.; Le Fur, Y.; Juen, P.; Masson, P.; Nicoud, J.-F.; Masse, R. *Chem. Mater.* **2000**, *12*, 1025–1033. (j) Wolff, J. J.; Siegler, F.; Matschiner, R.; Wortmann, R. *Angew. Chem., Int. Ed.* **2000**, *39*, 1436–1439. (k) Brunel, J.; Ledoux, I.; Zyss, J.; Blanchard-Desce, M. *Chem. Commun.* **2001**, 923–924. (l) Cho, B. R.; Lee, S. J.; Lee, S. H.; Son, K. H.; Kim, Y. H.; Doo, I.-Y.; Lee, G. J.; Kang, T. I.; Lee, Y. K.; Cho, M.; Jeon, S.-J. *Chem. Mater.* **2001**, *13*, 1438–1440. (m) Cho, B. R.; Park, S. B.; Lee, S. J.; Son, K. H.; Lee, S. H.; Lee, M.-J.; Yoo, J.; Lee, Y. K.; Lee, G. J.; Kang, T. I.; Cho, M.; Jeon, S.-J. *J. Am. Chem. Soc.* **2001**, *123*, 6421–6422.
- (15) The only supramolecular self-organization examples described in the literature for octupolar compounds concern crystal engineering or liquid crystals. For crystal engineering examples, see: (a) Zyss, J.; Brasselet, S.; Thalladi, V. R.; Desiraju, G. R. *J. Chem. Phys.* **1998**, *109*, 658–669. (b) Thalladi, V. R.; Brasselet, S.; Weiss, H.-C.; Bläser, D.; Katz, A. K.; Carrell, H. L.; Boese, R.; Zyss, J.; Nangia, A.; Desiraju, G. R. *J. Am. Chem. Soc.* **1998**, *120*, 2563–2577. (c) Evans, R.; Lin, W. *Acc. Chem. Res.* **2002**, *35*, 511–522. For liquid crystals see: (d) Omenat, A.; Barbera, J.; Serrano, J. L.; Houbrechts, S.; Persoons, A. *Adv. Mater.* **1999**, *11*, 1292–1295. (e) Kang, S. H.; Kang, Y.-S.; Zin, W.-C.; Olbrechts, G.; Wostyn, K.; Clays, K.; Persoons, A.; Kim, K. *Chem. Commun.* **1999**, 1661–1662.
- (16) (a) Sénéchal, K.; Maury, O.; Le Bozec, H.; Ledoux, I.; Zyss, J. *J. Am. Chem. Soc.* **2002**, *124*, 4561–4562. (b) Renouard, T.; Le Bozec, H.; Ledoux, I.; Zyss, J. *Chem. Commun.* **1999**, 871–872. (c) Le Bozec, H.; Renouard, T. *Eur. J. Inorg. Chem.* **2000**, 229–239. (d) Dhenaut, C.; Ledoux, I.; Samuel, I. D. W.; Zyss, J.; Bourgault, M.; Le Bozec, H. *Nature* **1995**, *374*, 339–342.

- (17) Lehn, J.-M. *Supramolecular Chemistry: Concept and Perspective 1st ed.* VCH, Weinheim **1995**.
- (18) (a) Schubert, U. S.; Eschbaumer, C. *Angew. Chem., Int. Ed. Engl.* **2002**, *41*, 2893–2925. (b) Newkome, G. R.; He, E.; Moorefield, C. N. *Chem. Rev.* **1999**, *99*, 1689–1746. (c) Constable, E. C. *Chem. Commun.* **1997**, 1073–1080.
- (19) Le Bozec, H.; Renouard, T.; Bourgault, M.; Dhenaut, C.; Brasselet, S.; Ledoux, I.; Zyss, J. *Synth. Met.* **2001**, *124*, 185–189.
- (20) Treaway, J. A.; Meyer, T. J. *Inorg. Chem.* **1999**, *38*, 2267–2278.
- (21) For preliminary communications see: (a) Le Boudier, T.; Maury, O.; Le Bozec, H.; Ledoux, I.; Zyss, J. *Chem. Commun.* **2001**, 2430–2431. (b) Le Bozec, H.; Le Boudier, T.; Maury, O.; Bondon, A.; Ledoux, I.; Deveau, S.; Zyss, J. *Adv. Mater.* **2001**, *13*, 1677–1681.
- (22) For other examples of polymers featuring octupolar chromophores see: (a) Cherix, F.; Maillotte, H.; Audebert, P.; Zyss, J. *Chem. Commun.* **1999**, 2083–2084. (b) Cho, B. R.; Chajara, K.; Oh, H. J.; Son, K. H.; Jeon, S.-J. *Org. Lett.* **2002**, *4*, 1703–1706. (c) Cho, B. R.; Piao, M. J.; Lee, S. H.; Yoon, S. J.; Jeon, S.-J.; Cho, M. *Chem. Eur. J.* **2002**, *8*, 3907–3916.

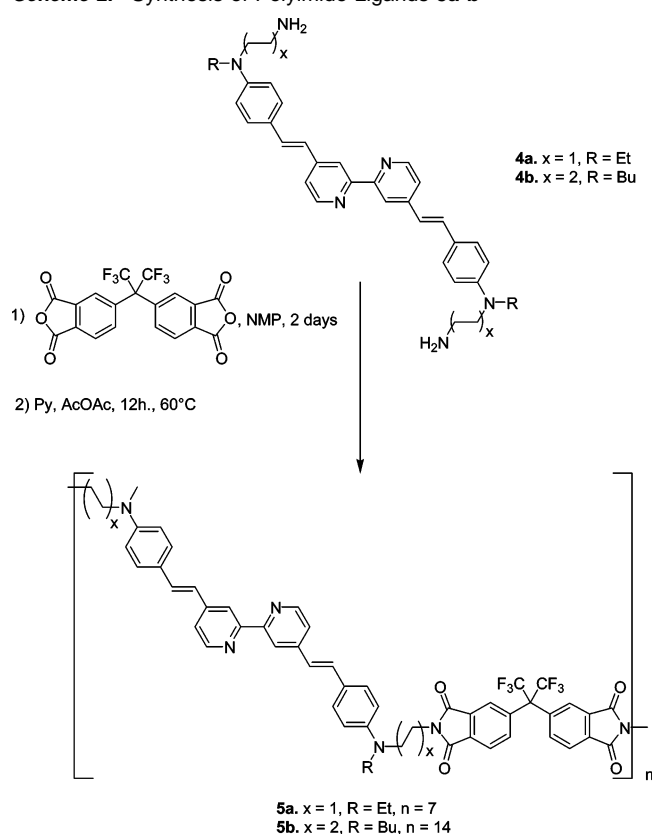
Scheme 1. Synthesis of Monomer. (i) Phthalimide (2eq)/PPh₃ (2eq) /DEAD (2eq), THF, Rt, 15h; (ii) N₂H₄ (10eq) THF, Reflux, 15h**Table 1.** Optical and Thermal Properties of Polymer Ligand 5a,b and Their Precursors 1–4a,b

compd	$\lambda_{\text{max}}/\text{nm}^a$	$\epsilon/\text{L.mol}^{-1}.\text{cm}^{-1}$	$\lambda_{\text{em}}/\text{nm}^a$	$T_{\text{d5}}/^\circ\text{C}^b$
1a	397	57000	495	340
1b	401	65000	497	355
3a	391	70000	480	
3b	400	57000	493	
4a	384	43000	499	
4b	400	38000	500	
5a	388		466	374
5b	397		472	398

^a Measured in dichloromethane. ^b Decomposition temperature at 5% weight loss determined by TGA.

received a great deal of attention because of their high thermal stability and high glass temperature (T_g). NLO polyimides are generally prepared via a polycondensation reaction of a diamino functionalized NLO-phore with a dianhydride. Therefore, to achieve the synthesis of the desired main-chain polyimides, the preparation of the proper diamino-substituted 4,4'-bis(dialkylaminostyryl)-[2,2']-bipyridine ligands was undertaken. The synthesis of the starting dihydroxy functionalized 4,4'-dialkylaminostyryl-[2,2']-bipyridines **2a** and **2b** has been previously reported.²³ Treatment of **2a,b** with phthalimide under Mitsunobu conditions (diethyl azodicarboxylate/triphenylphosphine) in THF at room temperature led to the formation of phthalimido derivatives **3a,b** (Scheme 1). Hydrazinolysis of **3a,b** in refluxing THF afforded the desired diamino-functionalized compounds **4a,b** in 94 and 92% yield, respectively.²⁴ All these precursors were fully characterized by ¹H NMR, absorption and emission spectroscopies, high resolution mass spectrometry and gave satisfactorily microanalysis. The comparison of their spectroscopic data with those of the parent ligands **1a,b**²⁵ clearly shows that the chromophoric structure is not affected during the reaction pathway (See the Supporting Information and Table 1).

As the choice of the dianhydride monomer has a strong influence on the solubility of the resulting polymers, we have

Scheme 2. Synthesis of Polyimide Ligands 5a–b

selected hexafluoroisopropylidene diphthalic anhydride (6FDA) which is known to enhance the polymer solubility with still high T_g . Polyimides **5a,b** were prepared by a two step synthesis consisting in: (i) a room-temperature polycondensation between **4a,b** and 6FDA in 1-methyl-2-pyrrolidinone (NMP) followed by (ii) an in-situ chemical imidization promoted by a pyridine/acetic anhydride mixture (Scheme 2).²⁶ The resulting brown-yellow polymers are soluble in chlorinated and in polar solvents

(23) Le Boudier, T.; Viau, L.; Guégan, J.-P.; Maury, O.; Le Bozec, H. *Eur. J. Org. Chem.* **2002**, 3024–3033.

(24) (a) Liang, Z.; Dalton, L. R.; Garner, S. M.; Kalluri, S.; Chen, A.; Steier, W. H. *Chem. Mater.* **1995**, 7, 941–944.

(25) Maury, O.; Guégan, J.-P.; Renouard, T.; Hilton, A.; Dupau, P.; Sandon, N.; Toupet, L.; Le Bozec, H. *New J. Chem.* **2001**, 25, 1553–1566.

(26) (a) Kenis, P. J. A.; Noordman, O. F. J.; van Hulst, N. F.; Engbersen, J. F. J.; Reinhoudt, D. N.; Hams, B. H. M.; van der Vorst, C. P. J. M. *Chem. Mater.* **1997**, 9, 596–601. (b) Yu, D.; Gharavi, A.; Yu, L. *J. Am. Chem. Soc.* **1995**, 117, 11 680–11 686.

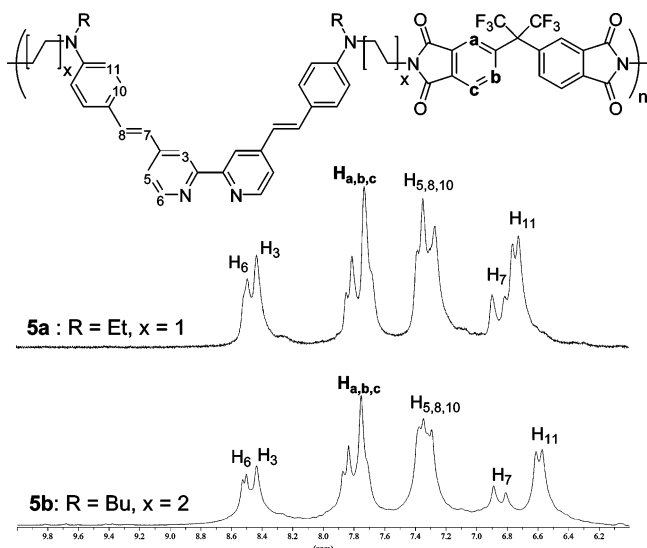


Figure 1. Aromatic part of the ^1H NMR spectra of polyimides **5a,b**.

Table 2. Molecular Weights and Glass Transition Temperature of Polyimides **5a–b**

polymer	Mw/Da	Mn/Da	PDI	N	$T_g/^\circ\text{C}$
5a	9300	6600	1.40	7	210
5b	19300	14100	1.37	14	165

(CH_2Cl_2 , THF, DMF, NMP). Gel permeation chromatography in THF (polystyrene as standard) gave relatively low molecular weights, indicating an average of ca. 7 and 14 bipyridyl units in **5a** and **5b**, respectively (Table 2). This difference can be explained by the enhanced solubility of monomer **4b** featuring butyl groups as compared to that of **4a** featuring ethyl end groups.

Both polymers were fully characterized by ^1H and ^{19}F NMR, FTIR, absorption and emission spectroscopies, and elemental analysis. Their ^1H NMR spectra (the aromatic part is depicted in Figure 1) displays two types of signals. The characteristic peaks of the dialkylaminostyryl-[2,2']-bipyridine moieties, assigned by analogy with the model chromophores **1a–b**,²⁵ clearly indicate that the chromophoric structure remains intact in the polymer. For example, the *trans* conformation of the styryl double bands is clearly established by the 3J coupling constant ($J_{\text{CH}=\text{CH}} = 16.1$ Hz). In addition, the spectrum exhibits a second set of signals between 7.6 and 8 ppm, which can be assigned to the aromatic protons $\text{H}_{\text{a,b,c}}$ of the phthalimide moieties. The absence of downfield signal corresponding to the polyamic acid proton suggests that the imidization led to completion. Moreover, the aliphatic methylene protons connected to the amino group in **4a,b** (2.92 and 2.72 ppm, respectively) are downfield shifted to 3.86 and 3.69 ppm in the polymer **5a,b** indicating the complete transformation of the amino into imido functions during the polymerization process.²⁷

The FTIR spectra of polyimides **5a,b** exhibit two characteristic $\nu_{\text{C}=\text{O}}$ vibration bands at ca. 1780 and 1720 cm^{-1} and one corresponding to the polyimide ring at 740 cm^{-1} .²⁸ In addition,

the typical polyamic acid vibration band at 1676 cm^{-1} is not observed, confirming again their complete conversion into polyimide. The absorption and emission spectra of **5a,b** (Table 1) display broad, intense and structureless intra-ligand charge-transfer transition (ILCT) at ca. 390 nm (λ_{abs}) and 470 nm (λ_{em}), similar to those of the parent ligands **1a,b**. Moreover, these bipyridine-polyimide ligands possess excellent thermal stability (Table 1) with 5% weight loss occurring above 370 $^\circ\text{C}$. Thermal analysis by DSC also shows high glass transition temperatures (T_g) at 210 $^\circ\text{C}$ for **5a** and 165 $^\circ\text{C}$ for **5b** (Table 2), as expected for NLO-polyimides. It is worth noting that the T_g of **5b** is significantly lower than that of **5a** ($\Delta T_g = 45$ $^\circ\text{C}$), in agreement with the more flexible structure of **5b** containing butyl linkers.

The sequential coordination ability of bipyridine ligands to ruthenium(II) has been used to achieve the synthesis of metallo-polyimides **7a** and **7b**. Bis(dialkylaminostyryl-[2,2']-bipyridyl) dichloro ruthenium complexes (alkyl = ethyl, **6a**; butyl, **6b**) were first prepared by refluxing $\text{RuCl}_3 \cdot 3\text{H}_2\text{O}$ and two equivalents of bipyridine **1a,b** in DMF in the presence of lithium chloride (Scheme 3). Final coordination of polymer ligands **5a,b** with **6a** and **6b** in refluxing DMF led to the almost quantitative formation (> 90%) of polymer complexes **7a,b**, isolated as their hexafluorophosphate or tris(tetrachlorobenzendiolate)phosphate (TRISPHAT)²⁹ salts, respectively (Scheme 3). The use of the TRISPHAT anion was found to greatly enhance the solubility of the resulting polymer in chlorinated solvents. The complete complexation of all bipyridyl units was established on the basis of ^1H NMR and UV–visible spectroscopy. In the ^1H NMR spectra, the signals at 8.51 (**5a**) and 8.53 ppm (**5b**) assigned to the H_6 protons of the bpy ligand (Figure 1) are upfield shifted upon complexation. As usually observed, the magnitude of this shift depends on the nature of the counteranion ($\Delta\delta = 1$ ppm for the PF_6 salt **7a**, $\Delta\delta = 0.5$ ppm for the TRISPHAT salt **7b**).^{29b} In addition, the UV–visible spectra of the polymer complexes **7a,b** display two maxima at 443 and 513 nm, characteristic of the overlapping ILCT and MLCT transitions respectively in the tris(dialkylaminostyryl-[2,2']-bipyridyl)ruthenium (II) complexes (vide supra). No shoulder at ca. 390 nm corresponding to the absorption maxima of the free polymer ligands **5a,b** could be observed, confirming the complete coordination of all bipyridyl subunits. In addition, it is worth noting that this new metallo-polymers displays very high thermal stability with $T_{\text{d}5} = 350$ $^\circ\text{C}$ and 358 $^\circ\text{C}$ for **7a** and **7b**, respectively.

(b) Controlled Polyoctupolar Architecture. In contrast to polyimides, metallo-dendrimers possess a discrete and well-controlled architecture. These macromolecules can be considered as an ordered ensemble of monomeric building blocks and their geometry can be predetermined by the nature of the connectivity. For that purpose we have designed multipodal ligands containing two (dipod) or three (tripod) dialkylaminostyryl-[2,2']-bipyridine chromophores, precursors to poly-octupoles based on tris(bipyridyl)ruthenium units.

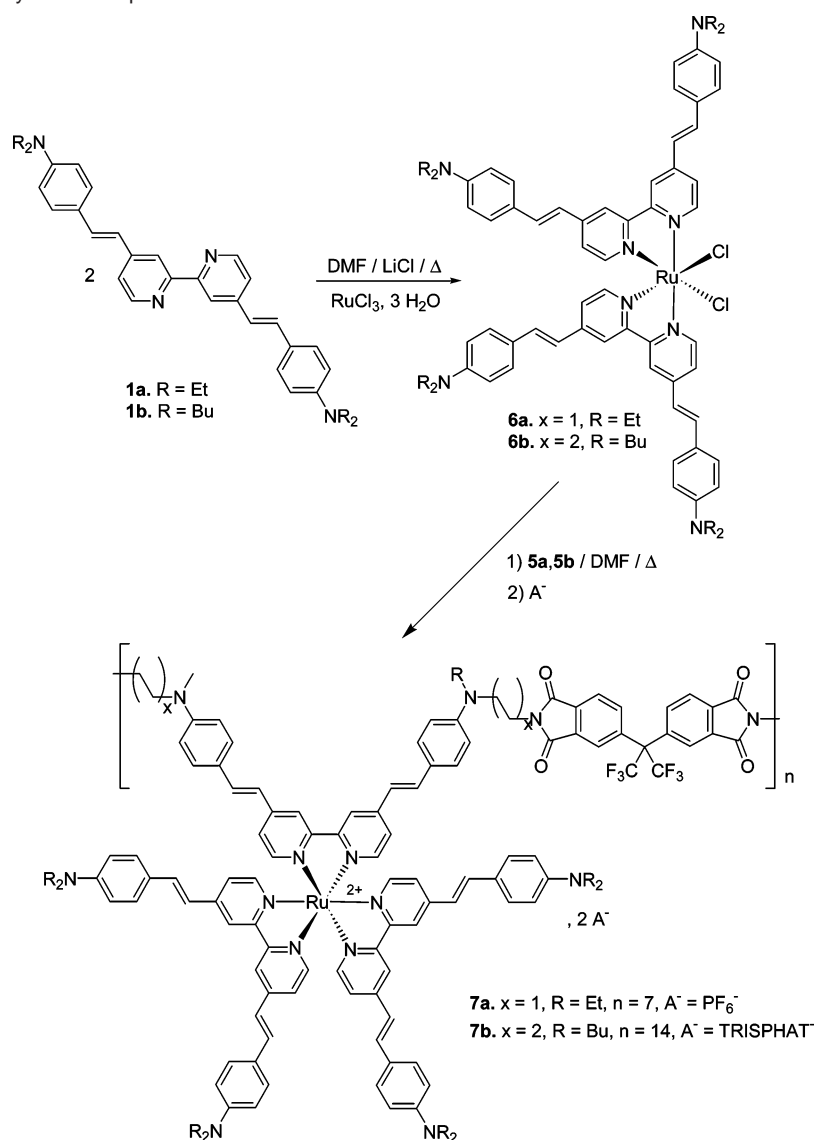
Dipod (**8**) and tripod (**9**) ligands were readily prepared by a nucleophilic substitution between monohydroxy functionalized 4,4'-bis(dialkylaminostyryl)-[2,2']-bipyridine **2c**²³ and α,α' -dibromo-*p*-xylene and 2,4,6-tris(bromomethyl)mesitylene, respectively, in the presence of sodium hydride in DMF (Scheme

(27) These chemical shifts are similar to those of the phthalimide functionalized bipyridine intermediates, i.e. 3.88 and 3.71 ppm for **3a** and **b**, respectively. In addition such 0.9 ppm shift has already been described by Kenis et al., see ref (26a).

(28) Perry, R. J. R.; Tunney, S. E.; Wilson, B. D. *Macromolecules* **1996**, *29*, 1014–1020.

(29) (a) Lacour, J.; Glinglinger, C.; Grivet, C.; Bernardelli, G. *Angew. Chem., Int. Ed. Engl.* **1997**, *36*, 608–610. (b) Maury, O.; Lacour, J.; Le Bozec, H. *Eur. J. Inorg. Chem.* **2001**, 201–204 and references therein.

Scheme 3. Synthesis of Polyimide Complexes 7a-b



4). Both multipodal ligands were fully characterized by ^1H , ^{13}C NMR, UV–visible spectroscopy, high-resolution mass spectrometry and elemental microanalysis. Their ^1H NMR spectra exhibit typical signals assigned to the bipyridyl units and to the central core, with for example characteristic benzylic (**8**, $\delta_{\text{CH}_2} = 4.48$ ppm; **9**, $\delta_{\text{CH}_2} = 4.53$ ppm) and mesitylenic (**9**, $\delta_{\text{CH}_3} = 2.36$ ppm) protons. The ^{13}C NMR spectra (Table 3 and the Experimental Section) clearly indicate the unsymmetrical nature of these ligands with two and three sets of signals for the styryl moieties ($\text{C}_4\text{--C}_{12}/\text{C}_{4'}\text{--C}_{12'}$, Table 3) and dialkylamino fragments ($\text{C}_{13}, \text{C}_{14}/\text{C}_{13'}, \text{C}_{14'}/\text{C}_{13'}$, $\text{C}_{14''}$), respectively. FAB-mass spectrometry shows weak peaks corresponding to the molecular ions and strong peaks due to fragmentations of the alkyl amino ether link. The UV–visible spectra of **8** and **9** exhibit classical ILCT transitions centered at 395 nm (Table 4). The oscillator strengths follow a 1/1.9/2.7 ratio for **2c**, **8**, **9**, respectively, as expected for non interacting sub-chromophores (1/2/3).^{14b,e}

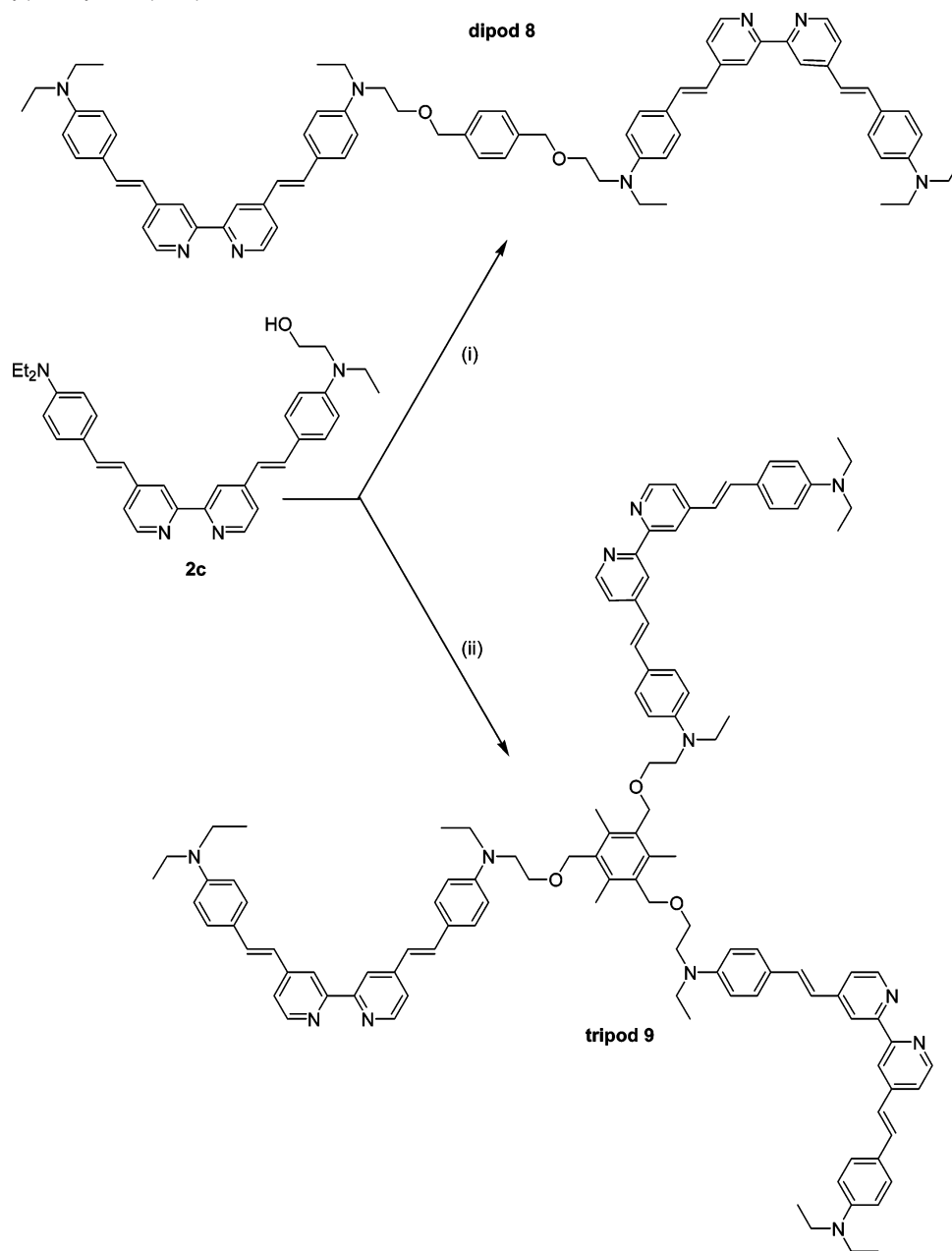
Reaction of $(\text{1a})_2\text{RuCl}_2$ **6a** with dipod **8** and tripod **9** in refluxing DMF led to the formation of deep red bimetallic (dimer **11**) and trimetallic (trimer **12**) complexes, after precipitation as their TRISPHAT salts (Figures 2 and 3). As for polymer **7b**, this anion greatly enhances the solubility of the polymetallic

complexes and allows their purification by silica gel column chromatography with dichloromethane as eluent.

Both complexes were characterized by NMR spectroscopy and gave satisfactorily elemental analysis. Unfortunately, mass spectrometry measurements did not allow the determination of the molecular ion exact mass and only fragmentations were observed (see the Experimental section). However, their structures could be confirmed by ^1H and ^{13}C NMR, by using COSY experiments for the determination of proton connectivities and HMBC and HMQC sequences for the assignment of C–H and quaternary carbons, respectively. Despite the presence of many possible diastereoisomers, owing to the chiral nature (Λ and Δ) of $(\text{bipy})_3\text{Ru}^{2+}$ and TRISPHAT^- , the NMR spectra of **11** and **12** show only one set of signals. The simplicity of the NMR spectra can be explained by (i) the homochiral self-assembling between racemic $(\text{1a})_3\text{Ru}(\text{II})$ **10** and TRISPHAT^- ions,^{29b} and (ii) the length of the spacer and thus the large distance between the chiral metal centers.³⁰ The complete coordination was clearly

(30) (a) Ishow, E.; Gourdon, A.; Launay, J.-P.; Chiorboli, C.; Scandola, F. *Inorg. Chem.* **1999**, *38*, 1504–1510. (b) Wärnmark, K.; Baxter, P. N. W.; Lehn, J.-M. *Chem. Commun.* **1999**, 993–994. (c) Kaes, C.; Hosseini, M. W.; De Cian, A.; Fischer, J. *Tetrahedron Lett.* **1997**, *38*, 3901–3904.

Scheme 4. Synthesis of Polypyridyl Ligands **8** and **9**, (i) NaH, DMF, α,α' -dibromo-*p*-xylene, (94%); (ii) NaH, DMF, 2,4,6-(tribromomethyl)Mesitylene, (96%)



established by the quantitative 0.5 ppm upfield shift of the resonance signal corresponding to the H_6 protons and by 2/1 and 3/1 integration ratio between the H_3 and benzylic H_{15} proton signals **11** and **12**, respectively. The ^{13}C NMR spectra of monomer **10**, dimer **11** and trimer **12** are very similar with chemical shift variations that do not exceed 0.1 ppm (Table 3). Note that the ^{13}C NMR signals are broader in the complexes as compared to those of free ligands, resulting in the overlap of signals belonging to the external bipyridine **1a** and to the multipodal ligands.

Multipodal bipyridyl ligands are well-known building blocks for the design of metallodendrimers with higher nuclearity^{18b,c} and the “metal as ligand”/“metal as complex” approach is an elegant strategy for the synthesis of such supramolecules.³¹ We

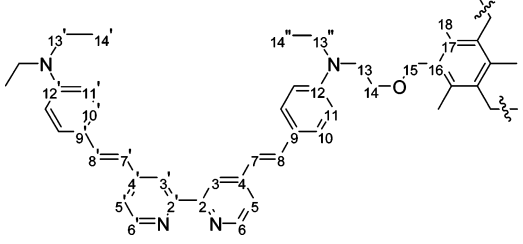
have applied this concept to design the first generation dendritic architecture featuring seven metallo-octupoles. The synthesis started with the preparation of the “metal as ligand” core $[\text{Ru}(\mathbf{9})_3][\text{TRISPHAT}]_2$ **13** by mixing $\text{RuCl}_2(\text{DMSO})_4$ with three equivalents of tripod **9** in refluxing DMF (Figure 4).

Side reactions such as the formation of bi- and tri-metallic compounds did not occurred since thin-layers chromatography did not reveal the presence of any free ligand. Such behavior has already been described for the synthesis of other “metal as ligand” core like $[\text{Ru}(\text{dpp})_3]^{2+}$ (dpp = bis(2-pyridyl)-pyrazine) reported by Denti, Campagna, Balzani and co-workers.^{32,33} NMR

(31) Balzani, V.; Campagna, S.; Denti, G.; Juris, A.; Serroni, S.; Venturi, M. *Acc. Chem. Res.* **1998**, *31*, 26–34.

(32) (a) Denti, G.; Campagna, S.; Serroni, S.; Ciano, M.; Balzani, V. *J. Am. Chem. Soc.* **1992**, *114*, 2944–2950. (b) Serroni, S.; Denti, G.; Campagna, S.; Juris, A.; Ciano, M.; Balzani, V. *Angew. Chem., Int. Ed. Engl.* **1992**, *31*, 1493–1495.

(33) In addition, the formation of *mer* and *fac* isomers can be envisaged on the basis of molecular mechanics simulation. No difference between these isomers could be detected by means of NMR spectroscopy.

Table 3. Atom Numbering and ^{13}C NMR Data of Compounds **9**–**14**


	carbon ^a (f or c)	tripod 9	monomer ^b 10	trimer ^b 12	13	heptamer ^b 14
f	2	156.81			156.70	
f	3	117.86			117.86	
f	4–4'	146.99–146.90			147.01–146.91	
f	5	120.60			120.64	
f	6	149.67			149.64	
f	7–7'	121.28–120.97			120.97	
f	8–8'	133.78–133.68			133.82	
f	9–9'	124.08–123.68			123.59	
f	10–10'	128.95–128.92			128.95	
f	11–11'	112.02–111.87			112.02–111.86	
f	12–12'	148.73–148.67			148.75–148.68	
c	2		157.29	157.36	157.27	157.30
c	3		120.03	120.21	120.10	120.13
c	4		147.42	147.55	147.47	147.46
c	5		122.61	122.72	122.47	122.63
c	6		151.37	151.11	151.18	151.36
c	7		117.67	117.78	(–)	117.69
c	8		136.73	136.92	136.84	136.61
c	9		122.87	122.95	122.78	(–)
c	10		129.79	129.81	129.76	129.81
c	11		111.76	110.93	(–)	111.76
c	12		149.43	149.39	(–)	149.44
f/c	13	50.59		50.53	50.59	50.59
f/c	13'	44.78	44.85	44.83	44.77	44.85
f/c	13''	45.88		45.84	45.87	45.82
f/c	14	68.62		68.42	68.36	68.67
f/c	14''	12.38		12.40	12.39	12.41
f/c	14'	12.80	12.81	12.84	12.81	12.84
f/c	15	68.38		68.65	68.61	68.67
f/c	16	138.40		138.37	138.41	138.36
f/c	17	133.17		133.10	133.02	133.08
f/c	18	15.94		15.92	15.94	15.94

^a f = carbon belonging to free ligand; c = carbon belonging to coordinated ligand. ^b Carbon belonging to the TRISPHAT anion are omitted for clarity.

Table 4. Spectroscopic, Photophysical and Thermal Properties of Multipodal Ligands and Corresponding Complexes

compd	$\lambda_{\text{abs}}/\text{nm}$ ($\epsilon/\text{L}\cdot\text{mol}^{-1}\cdot\text{cm}^{-1}$) ^a	$\lambda_{\text{em}}/\text{nm}$	ϕ_{em} ^c	$\tau/\mu\text{s}$ ^d	$T_{\text{d}}/^\circ\text{C}$ ^b
2c	389 (43000)	496 ^a			325
dipod 8	395 (90000)	497 ^a			366
tripod 9	396 (130000)	498 ^a			348
monomer	447 (146000)	708 ^c	4.15×10^{-3}	5.15	365
10	520 (143000)				
dimer	440 (258000)				325
11	511 (239000)				
trimer	443 (379000)	708 ^c	2.60×10^{-3}	4.14	328
12	511 (354000)				
heptamer	444 (693000)	708 ^c	1.85×10^{-3}	3.08	321
14	506 (648000)				

^a Measured in dichloromethane. ^b Decomposition temperature at 5% weight loss. ^c In MTHF. ^d In THF.

spectra (^1H and ^{13}C) exhibit the characteristic resonance signals of coordinated and free dialkylaminostyryl-[2,2']-bipyridine (Table 3). Moreover, in the ^1H NMR spectrum (Figure 5), an integration ratio of 0.65 (th. 0.66) between $\text{H}_{6\text{f}}$ and $\text{H}_{3\text{f}}+\text{H}_{3\text{c}}$ can be estimated after deconvolution of the corresponding

resonance signals, confirming the structure of **13**. Further evidence is given by the UV–visible spectrum (Figure 6) which exhibits a strong transition band of free chromophores ($\lambda = 400$ nm) and the characteristic $[(\mathbf{1a})_3\text{Ru}]^{2+}$ spectra ($\lambda_{\text{max}} = 518$ nm).

Finally, reaction of **13** with six equivalents of **6a** in refluxing DMF, followed by anionic exchange from chloride to TRISPHAT anion, led to the formation of the heptamer **14** in 91% yield (Figure 7). It is worth noting that this 14 cationic charged molecule was purified by chromatography column (silica gel-dichloromethane/methanol as eluent), thanks to the strong ion-pairing effect induced by the TRISPHAT anion. This reaction was monitored by UV–visible spectroscopy (Figure 6), clearly showing the disappearance of the 400 nm transition of the free bipyridyl ligand. The final spectrum is similar to that of $[(\mathbf{1a})_3\text{Ru}]^{2+}$ with a very broad, intense band (up to $690\,000\text{ L mol}^{-1}\text{ cm}^{-1}$) with two maxima at 444 and 506 nm due to the overlapping ILCT and MLCT transitions (Table 4).

^1H NMR signals of **14** are relatively broad, but integration ratio between H_3 and either benzylic H_{15} or mesitylenic H_{18} protons can be estimated to 2.32 (th. 2.33) and 1.47 (th. 1.55) respectively, confirming the heptametallal stoichiometry. ^{13}C NMR spectrum (Figure 8 and Table 3) is similar to those of **10**, **11**, and **12**; all the signals corresponding to the free bipyridyl ligands have disappeared. In addition, the elemental analysis shows that **14** precipitates with fourteen molecules of dichloromethane, a ratio confirmed by the integration of the solvent peak in the ^1H NMR spectrum.

II. Physical Properties

(a) Photophysical Properties. Substantial attention is currently devoted to polynuclear complexes and supramolecular architectures that are capable to absorb visible light and to luminesce in solution at room temperature in view of their potential utilization in many domains such as molecular electronics and artificial photosynthesis.³⁴ Of particular interest are the dendritic structures based on ruthenium complexes of polypyridine-type ligands.^{18,35} To examine the potential influence of dendritic structure on the photophysical behavior of the trimer **12** and the heptamer **14**, we have determined their emission properties in tetrahydrofuran (THF) or methyltetrahydrofuran (MTHF) solutions, using the monomer **10** and $[\text{Ru}(\text{bpy})_3]^{2+}$ as references. As observed for the polyimide compounds **7b**, the electronic absorption spectra of compounds **10**, **12**, and **14** (Figure 9, Table 4) exhibit in the visible region a band with two maxima at about 440 and 510 nm (442 and 519 nm for the monomer in MTHF) attributed to ILCT and MLCT transitions, respectively. Whatever the excitation wavelength in the 300–600 nm range, the three compounds present a very similar emission spectrum with a maximum at the same

- (34) (a) Meyer, T. J. *Acc. Chem. Res.* **1989**, *22*, 163–170. (b) Balzani, V.; Scandola, F. *Supramolecular Photochemistry*, Ellis Horwood, New York, 1991. (c) Sauvage, J. P.; Collin, J. P.; Chambron, J. C.; Guillerez, S.; Coudret, C.; Balzani, V.; Barigelli, F.; De Cola, L.; Flamigni, L. *Chem. Rev.* **1994**, *94*, 993–1019. (d) Amouyal, E. *Sol. Energy Mater. Sol. Cells* **1995**, *38*, 249–276. (e) Amouyal, E. in *Homogeneous Photocatalysis*, Chanon, M. Ed., J. Wiley, Chichester, chapter 8, 1997; pp 263–307. (f) Konstantaki, M.; Koudoumas, E.; Couris, S.; Lainé, P.; Amouyal, E.; Leach, S. J. *Phys. Chem. B* **2001**, *105*, 10 797–10 804.
- (35) (a) Balzani, V.; Juris, A.; Venturi, M.; Campagna, S.; Serroni, S. *Chem. Rev.* **1996**, *96*, 759–833. (b) Newkome, G. R.; Patri, A. K.; Godinez, L. A. *Chem. Eur. J.* **1999**, *5*, 1445–1451 (c) Balzani, V.; Ceroni, P.; Juris, A.; Venturi, M.; Campagna, S.; Puntoriero, F.; Serroni, S. *Coord. Chem. Rev.* **2001**, *219–221*, 545–572.

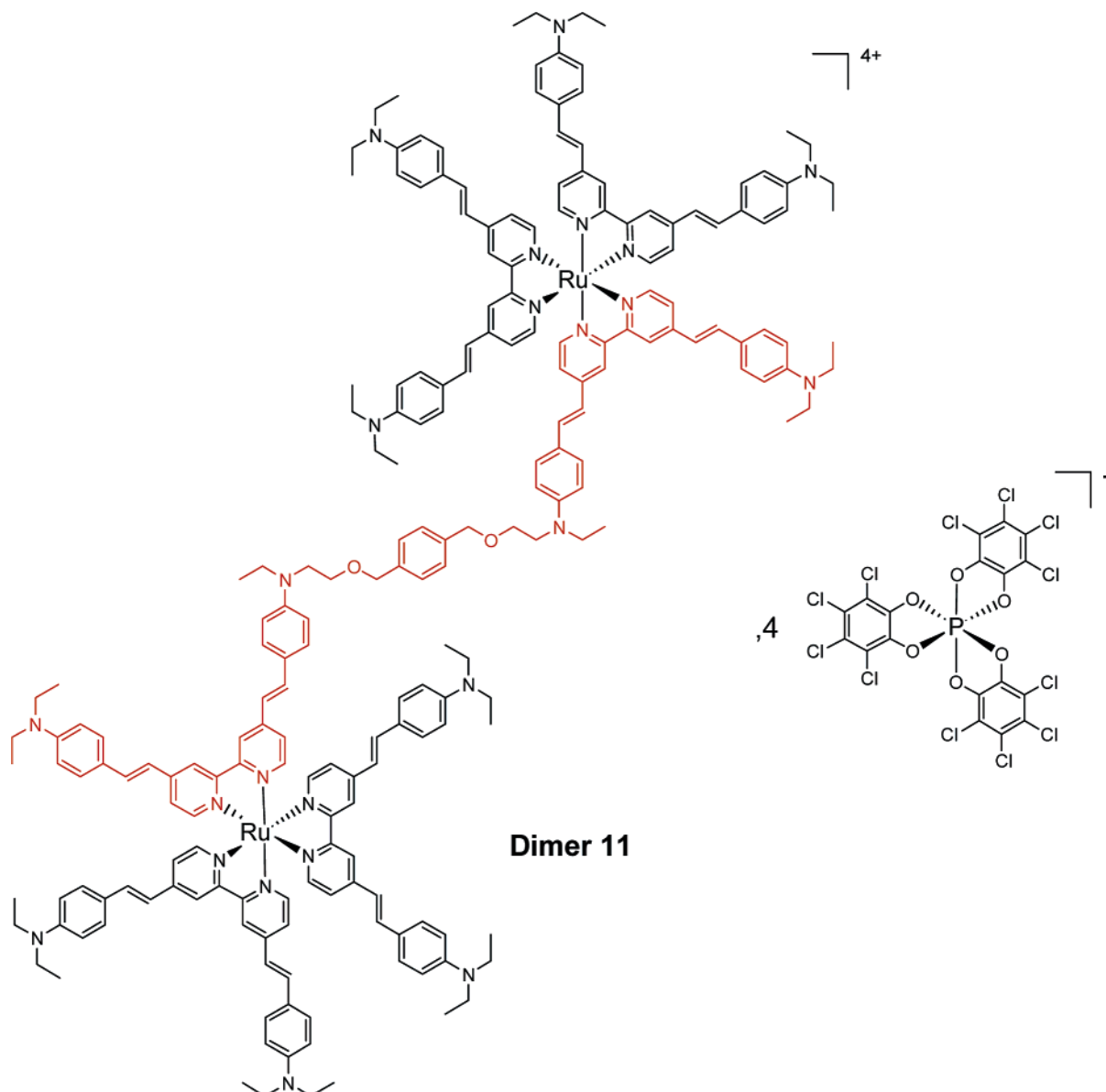


Figure 2. Chemical structure of bimetallic complex **11**.

wavelength i.e., 708 nm and a shoulder at about 780 nm more pronounced for the trimer **12** and the heptamer **14**. The luminescence excitation spectra, monitored at 708 nm, parallel the absorption spectra recorded over the visible region (maxima at 440 and 520 nm for **10**, 438 and 522 nm for **12**, 442 and 518 nm for **14** in MTHF), indicating that the observed emissions are clearly due to the Ru sites. The value of 708 nm ($14\,120\text{ cm}^{-1}$) for the emission maximum corresponds to a bathochromic shift of 2380 cm^{-1} with respect to $[\text{Ru}(\text{bpy})_3]^{2+}$. This shift is similar to that obtained for the luminescence of compounds **10**, **12**, and **14** to MLCT triplet states. The luminescence quantum yields ϕ_{em} determined for **12** and **14** are slightly lower than that for the monomer **10** and decrease as the number of metallic sites (N) increases (Table 4). The same trend is observed for the luminescence lifetimes τ (Table 4). As the energy of the excited triplet state (estimated from the maximum of the emission spectra) for the three compounds is nearly the same, the lowering of ϕ_{em} and τ , by a factor 2 in going from the mononuclear to the heptanuclear complex, is probably due to

the increase with N of nonradiative deactivation processes rather than to the quenching of the emitting triplet state by a metal-centered excited state located at higher energy, as usually put forward for polypyridine Ru complexes. In other words, and as also stressed by the similarity of the excitation spectra, the octahedral geometry around the metal sites is probably not distorted by the dendritic structure. It should be emphasized that the excited-state lifetime of $5.15\text{ }\mu\text{s}$ determined for the monomer in THF is very long and more than five times greater than that observed for $[\text{Ru}(\text{bpy})_3]^{2+}$ (930 ns in THF). This can be explained by the presence of the diethylaminostyryl conjugated substituents on bipyridine which extend the electronic delocalization over the entire DEASbpy ligand.³⁶ What is also remarkable for homometallic polynuclear complexes such as **12** and **14** is that their excited-state lifetime remains very long (4.14 and $3.08\text{ }\mu\text{s}$, respectively; Table 4).^{35a,37} This result offers interesting perspectives for the study of the photochemical

(36) Strouse, G. F.; Schoonover, J. R.; Duesing, R.; Boyde, S.; Jones W. E., Jr.; Meyer, T. J. *Inorg. Chem.* **1995**, *34*, 473–487.

(37) De Cola, L.; Belser, P. *Coord. Chem. Rev.* **1998**, *177*, 301–346.

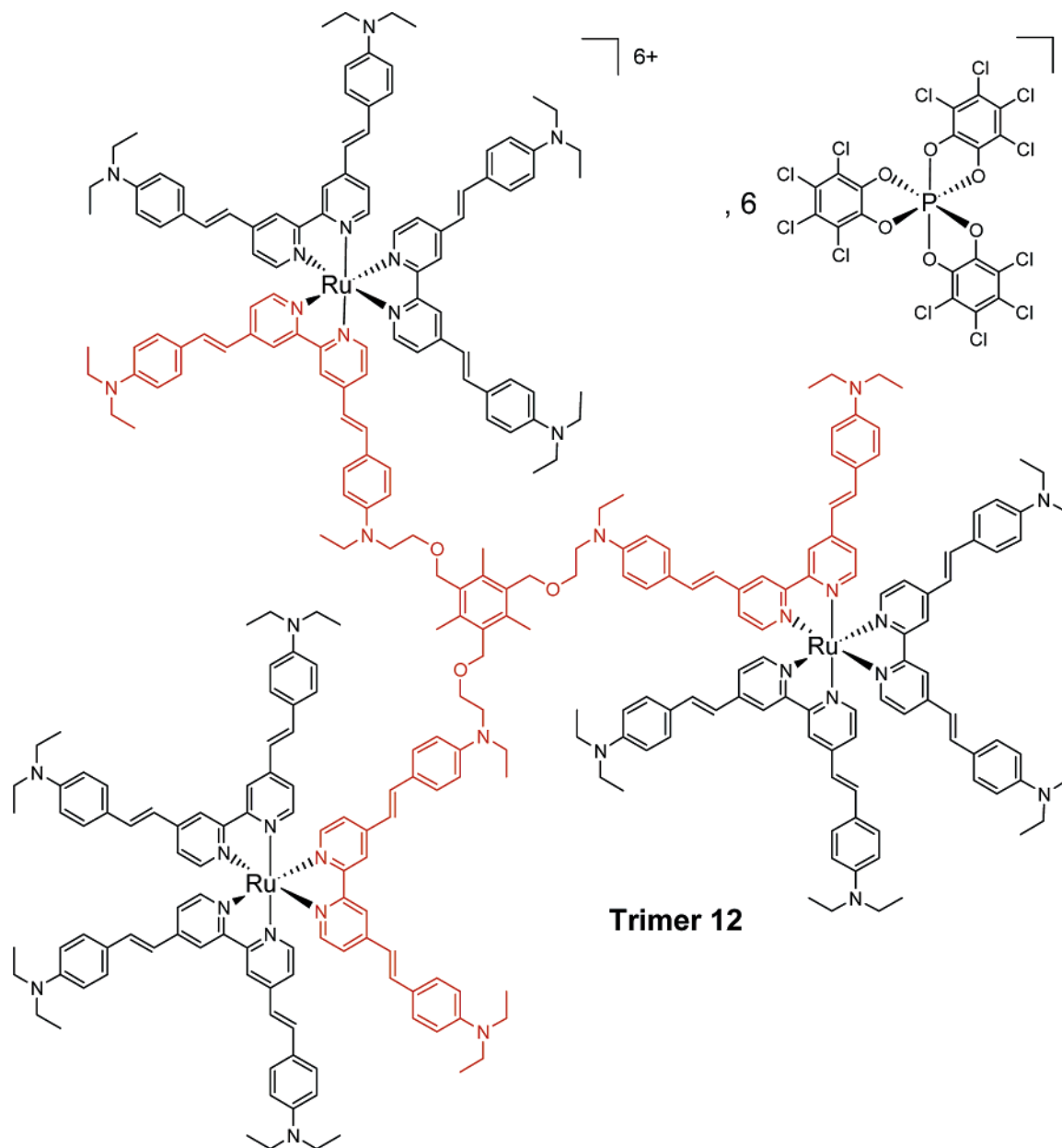


Figure 3. Chemical structure of trimetallic complex **12**.

reactivity of this kind of dendrimers—for example as potential multielectron-transfer elements—and for many applications. In particular, besides the NLO properties of these multi-octupolar compounds (vide infra), their long $^3\text{MLCT}$ lifetimes associated with a better overlapping of their absorption spectra with the solar spectrum as compared to $[\text{Ru}(\text{bpy})_3]^{2+}$ (red-shift of about 70 nm) make these complexes good candidates as components of model systems for photochemical and photoelectrochemical conversion of solar energy.

(b) NLO Properties. As EFISH experiment, which requires dipoles orientation in solution, is precluded for purely octupolar molecules, Harmonic Light Scattering³⁸ (HLS) technique was used for the molecular hyperpolarizability (β) measurements. Two-photon-induced fluorescence may significantly affects HLS measurements of $\text{Ru}(\text{bpy})_3^{2+}$ derivatives in the visible range,

leading to overestimation of hyperpolarizability values.³⁹ In the case of monomer **10**, previously uncorrected measurements at $\lambda = 1.34 \mu\text{m}$ for the fundamental wavelength provided a $\beta^{1.34}$ value of 2200×10^{-30} esu.^{16d} Improvements in the harmonic filtering system allowed to reduce the parasite fluorescence emission, thus yielding a corrected $\beta^{1.34}$ value of 1130×10^{-30} esu.¹⁹ The difference between uncorrected and corrected values confirms the importance of the multiphoton fluorescence contribution. New β measurements at the infrared shifted $\lambda = 1.91 \mu\text{m}$ fundamental wavelength were performed as the second harmonic wavelength at 955 nm lies in the transparency region of the chromophores, then making any contribution from two-photon fluorescence to HLS signal quite negligible. Indeed, $\beta^{1.91} = 320 \times 10^{-30}$ esu for **10** (Table 5) is far below the β value inferred from HLS measurements at $1.34 \mu\text{m}$, then confirming the large two-photon fluorescence contribution to the HLS signal

(38) (a) Terhune, R. W.; Maker, P. D.; Savage, C. M. *Phys. Rev. Lett.* **1965**, *14*, 681–684. (b) Clays, K.; Persoons, A. *Phys. Rev. Lett.* **1991**, *66*, 2980–2983.

(39) Morrison, I. D.; Denning, R. G.; Laidlaw, W. M.; Stammers, M. A. *Rev. Sci. Instrum.* **1996**, *67*, 1445–1453.

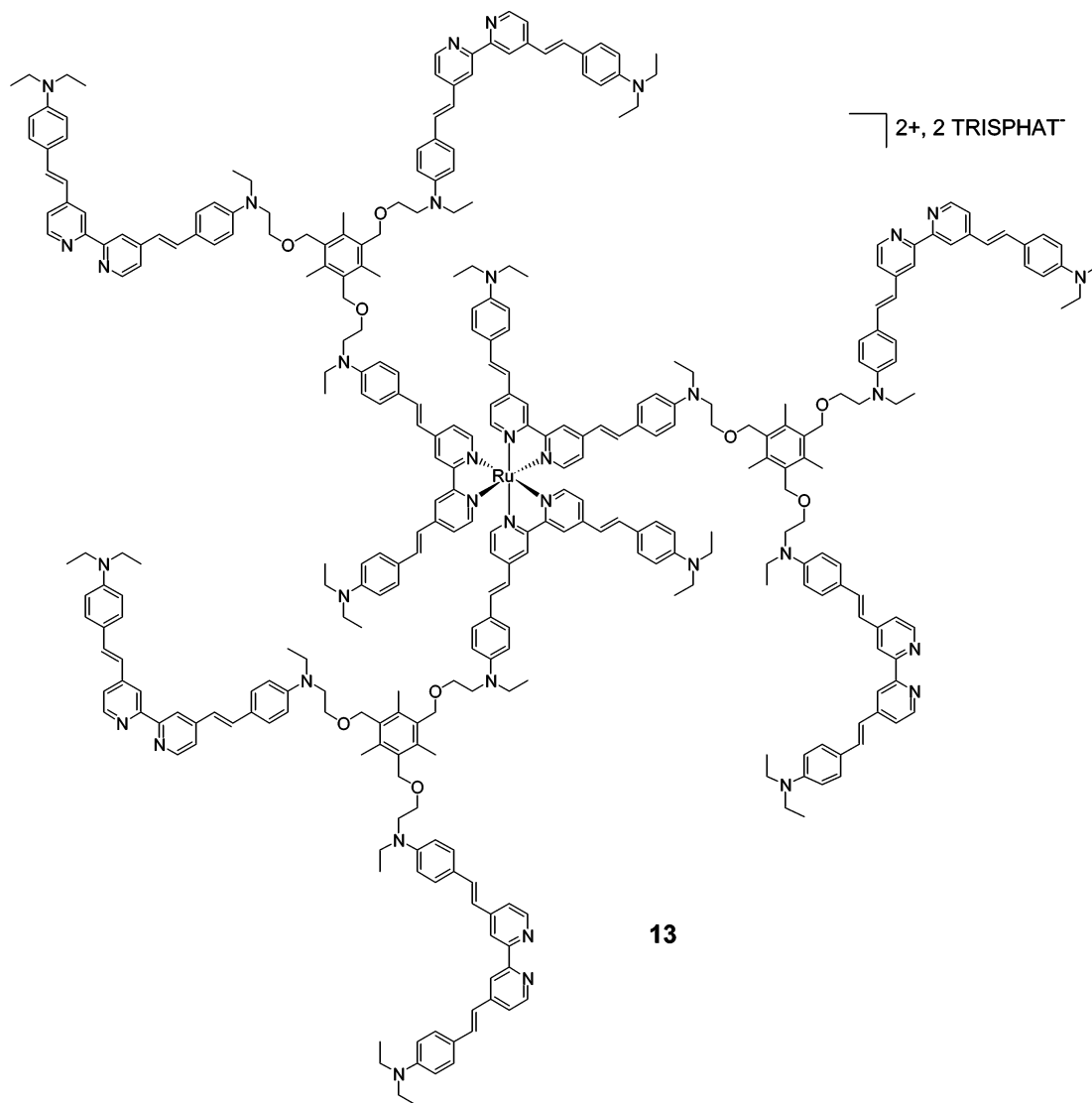


Figure 4. Chemical structure of $[(\text{tripod})_3\text{Ru}][\text{TRISPHAT}]_2$ **13**.

in the visible range. Therefore, the $\beta^{1.91}$ values reported herein can be considered as a fluorescence-free.

Calculation of the static β_0 value of monomer **10** is difficult as the two ILCT and MLCT transitions may contribute to the first hyperpolarizability.⁴⁰ Nevertheless, it can be roughly estimated from the two levels model using the more red-shifted transition.⁴¹ It is worth noting that this underestimated value of 208×10^{-30} esu still remains very large, in the same order of magnitude as the analogous zinc complex [$\lambda_{\text{max}} = 466$ nm, $\beta^{1.91} = 340 \times 10^{-30}$ esu, $\beta_0 = 241 \times 10^{-30}$ esu].^{16a} It is significantly higher than those of the most efficient organic chromophores such as 1,3,5-triscyano-2,4,6-tris(dibutylaminobisteryl)benzene^{14l,m} [$\lambda_{\text{max}} = 470$ nm, $\beta^{1.56} = 219 \times 10^{-30}$ esu, $\beta_0 = 116 \times 10^{-30}$ esu], 1,3,5-tris(methylsulfonylbisteryl)benzene^{14k} [$\lambda_{\text{max}} = 377$ nm, $\beta^{1.34} = 250 \times 10^{-30}$ esu, $\beta_0 = 157 \times 10^{-30}$ esu] and 4,9,14-

tris-(4'-(di-4-methoxyphenyl)aminophenylethynyl)truxen-one^{14b} [$\lambda_{\text{max}} = 509$ nm, $\beta_0^{\text{xxx}} = 169 \times 10^{-30}$ esu, $\beta_0 = 104 \times 10^{-30}$ esu].

The $\beta^{1.91}$ values of multimetallic species **7**, **11**, **12**, and **14** can be rigorously compared to that of **10** because (i) all these species exhibit very similar absorption spectra (vide supra) and (ii) all the HLS measurements were performed under similar monomer concentration in dichloromethane solution. Table 5 summarizes the NLO data for the whole family of complexes featuring from 1 to 14 octupolar elementary building-blocks. The NLO activity increases from monomer to dimer ($N = 2$), trimer ($N = 3$) and heptamer ($N = 7$), but decreases from heptamer to polymer ($N = 14$). The β_0 value of heptamer **14** (1271×10^{-30} esu) is the highest ever measured for an octupolar compound and within the same range as that of the most efficient dipolar polyenic molecule [$\lambda_{\text{max}} = 826$ nm, $\beta_0 = 1470 \times 10^{-30}$ esu].⁴² However, it still remains significantly lower than the β value of a recently reported multichromophoric dipolar dendron made of 15 azobenzene NLO-phores [$\lambda_{\text{max}} = 475$ nm, $\beta_0 = 3857 \times 10^{-30}$ esu].^{12b}

(40) For an evaluation to the contribution of each transition to the total NLO-activity of **10** see: Vance, F. W.; Hupp, J. T. *J. Am. Chem. Soc.* **1999**, *121*, 4047–4053.

(41) The two levels model allows the determination of nonresonant molecular hyperpolarizability β_0 according to $\beta_0/\beta = (\omega_{\text{max}}^2 - \omega^2)(\omega_{\text{max}}^2 - 4\omega^2)/\omega_{\text{max}}^4$, where ω is the frequency of the incident photon and ω_{max} is the absorption maximum frequency of the studied molecule. Oudar, J. L. *J. Chem. Phys.* **1977**, *67*, 446–457.

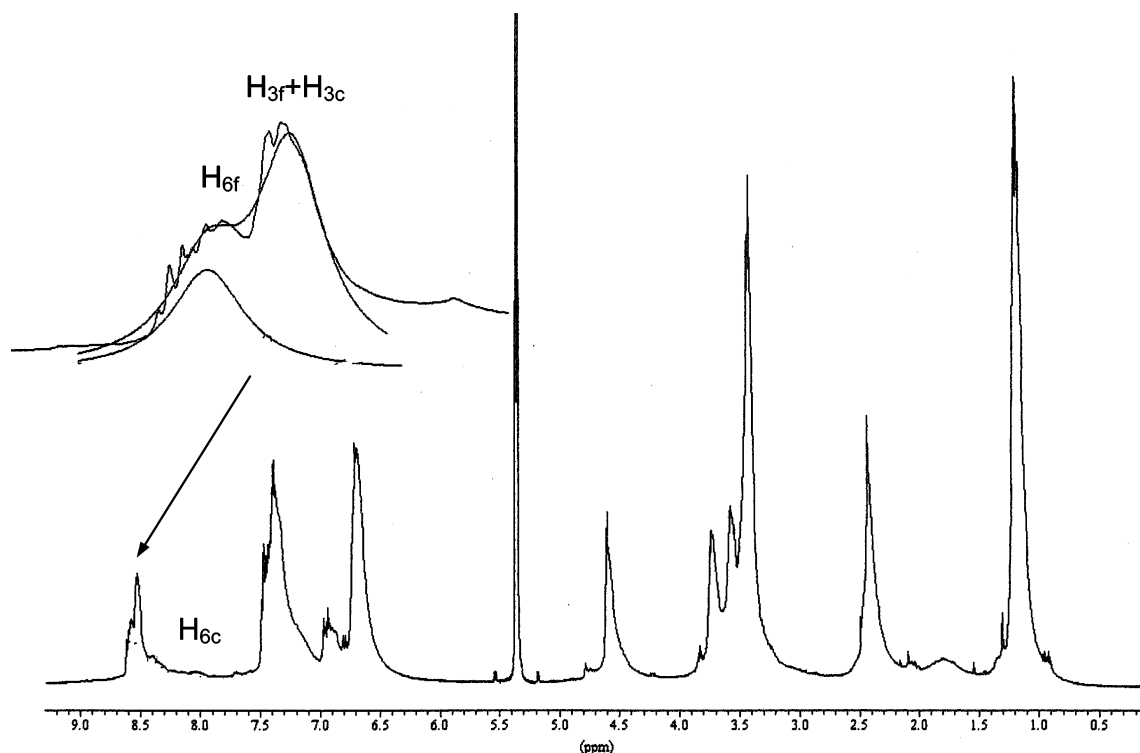


Figure 5. ^1H NMR spectrum (500 MHz, CD_2Cl_2 , 298 K) of complex **13** with deconvolution of the signals assigned to H_{6c} and $\text{H}_{3c} + \text{H}_{3f}$.

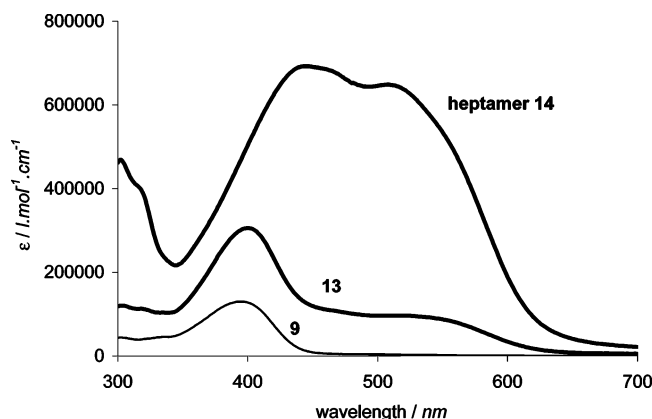


Figure 6. UV-visible monitoring for the synthesis of heptamer **14**.

The HRS intensity of a supramolecular architecture containing N monomeric subunits $I_{2\omega}(N)$ is given by the eq 1

$$I_{2\omega}(N)/I_{2\omega}(\text{ref}) = G \cdot [n_s \cdot \langle \beta_s^2 \rangle + n_{\text{supra}} \cdot \langle \beta_{\text{supra}}^2 \rangle] \quad (1)$$

where $I_{2\omega}(\text{ref})$ is the second harmonic intensity of a reference compound (NPP, see Supporting Information), n_s and n_{supra} are the mole number of solvent and solute respectively, β_s and β_{supra} their first hyperpolarizability tensor, $\langle \beta_s^2 \rangle$ and $\langle \beta_{\text{supra}}^2 \rangle$ refer to the orientational average of the β_s , β_{supra} tensor product and G is a proportionality constant. In the following, β is defined as $\sqrt{\langle \beta^2 \rangle}$; owing to the high concentrations and large hyperpolarizability values of our molecules, the HLS contribution from the pure solvent can be neglected. When the supramolecule is made of N fully disordered monomers, the solution containing n_{supra} molecules can be considered as a disordered medium

containing $n_{\text{supra}} \cdot N$ monomers, and the corresponding HLS intensity is given by then

$$I^{2\omega} = G n_{\text{supra}} \langle \beta_{\text{supra}}^2 \rangle = G \cdot n_{\text{supra}} \cdot N \langle \beta(1)^2 \rangle \quad (2)$$

$$\beta_{\text{supra}}(N)/\beta(1) = \sqrt{N} \quad (3)$$

where $\beta(1)$ is the monomer ($N = 1$) first hyperpolarizability. The increase of $\beta_{\text{supra}}(N)$ is simply the result of a concentration effect. Figure 10 plots the ratio $\beta_{\text{supra}}(N)/\beta(1)$ as a function of the subunits number N . It appears clearly that polymer **7b** ($N \approx 14$) fits perfectly with eq 3; the experimental hyperpolarizability ratio is about 4.0 very close to the theoretical value $\sqrt{14} = 3.7$. Such agreement accounts for the fully disordered assembly of monomeric ruthenium building blocks in the linear polymeric chain.

A totally different behavior is observed for the heptamer **14** ($N = 7$) which exhibits a giant first hyperpolarizability of $\beta^{1.91-}(7) = 1900 \times 10^{-30}$ esu, although containing half the number of monomeric subunits as compared to **7b**. In that case, the first hyperpolarizability satisfactorily fits with a linear relationship (4), as illustrated by Table 5 and Figure 10

$$\beta_{\text{supra}}(N)/\beta(1) = N \quad (4)$$

Such quasi-linear dependence is the signature of a quasi-optimized ordering of the individual building blocks in the heptamer. In this configuration, the HLS intensity can be expressed as

$$I^{2\omega} = G n_{\text{supra}} \langle \beta_{\text{supra}}^2 \rangle = G \cdot n_{\text{supra}} \langle (N\beta(1))^2 \rangle \quad (5)$$

This means that in a highly ordered dendritic architecture, each monomeric subunits coherently contributes to the HLS response.

(42) Blanchard-Desce, M.; Alain, V.; Bedworth, P. V.; Marder, S. R.; Fort, A.; Runser, C.; Barzoukas, M.; Lebus, S.; Wortmann, R. *Chem. Eur. J.* **1997**, *3*, 1091–1104.

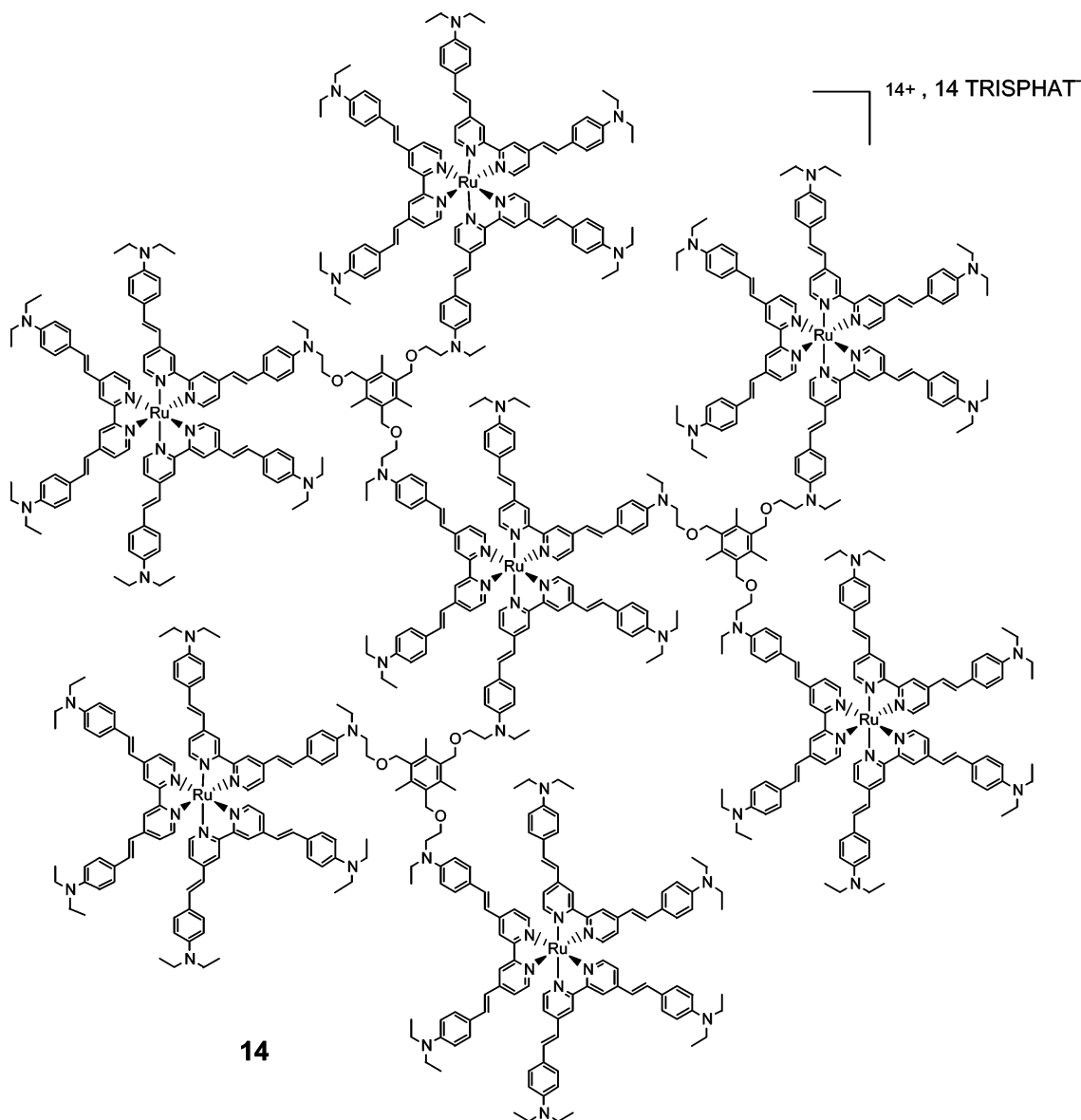


Figure 7. Chemical structure of the heptamer **14**.

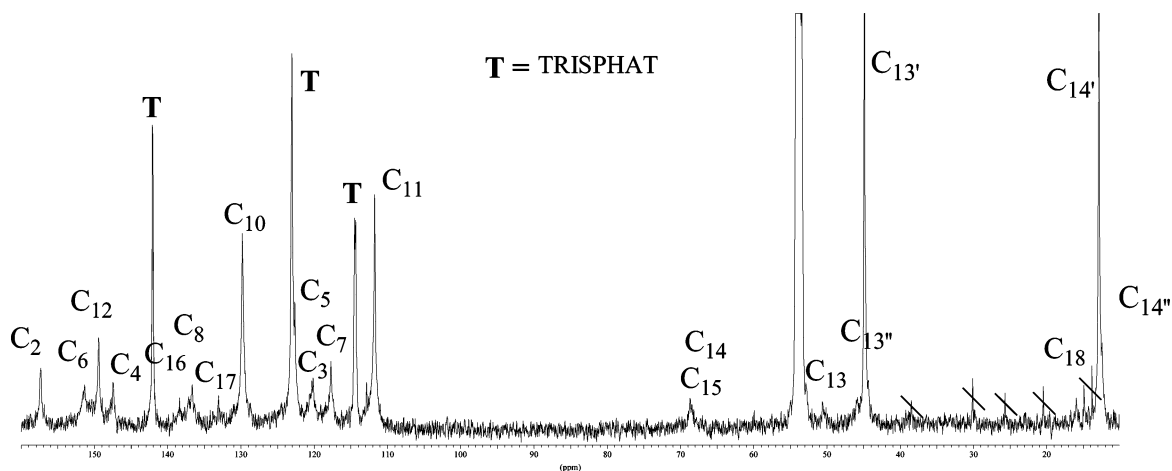


Figure 8. ^{13}C NMR spectrum of heptamer **14** in CD_2Cl_2 at 298 K.

In the cases of dimer **11** and trimer **12**, the experimental ratio $\beta(2)/\beta(1) = 1.8$ and $\beta(3)/\beta(1) = 2.2$ are intermediates between the two relationships described by equations (3) and (4).

However, the uncertainty inherent to HLS measurements ($\pm 20\%$) precludes the possibility to draw any firm conclusion as to supramolecular ordering in **11** and **12**.

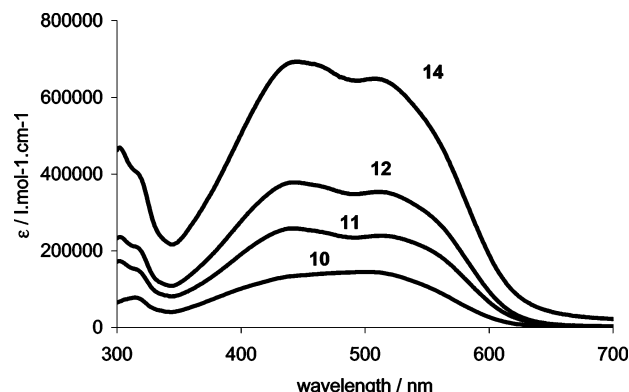


Figure 9. UV-visible spectra of poly-octupolar containing complexes.

Table 5. Nonlinear Optical Properties of the Poly Octupolar Complexes

compd	$\beta / 10^{-30}$ esu ^a	$\beta(N)/\beta(1)$	N	\sqrt{N}
monomer10	320	1	1	1
dimer11	570	1.8	2	1.41
trimer12	700	2.2	3	1.73
heptamer14	1900	5.9	7	2.65
polymer7b	1300	4.1	14	3.74

^a Measured by HLS at 1.91 μm (precision $\pm 20\%$). Correlation between esu and SI units: $\beta(\text{SI}) = 4.172 \times 10^{-10} \beta(\text{esu})$

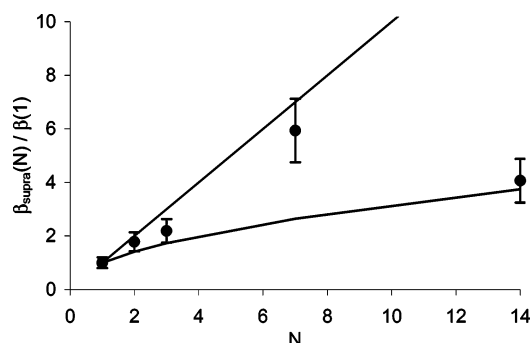


Figure 10. Plot of the ratio $\beta_{\text{supra}}(N)/\beta(1)$ vs. N .

A similar linear variation (eq 3) has already been described by Yokoyama and co-workers for dipolar NLO-phores included in a cone-shape dipolar dendritic architecture.^{12b} We report here the generalization of such behavior in the case of D_3 octupolar NLO-phores included in a dendritic architecture featuring the same D_3 global symmetry. To illustrate the supramolecular D_3 ordering, computer modeling of **14** was carried out on the basis of molecular mechanics calculation (MMF94). Projection of the heptamer structure along its C_3 axis (Figure 11) clearly suggests octupolar 3-fold symmetry at the supramolecular level. This fairly agrees with a recent STM imaging and molecular mechanics calculations on a heptanuclear ruthenium dendrimer.⁴³ Such octupolar arrangement of octupolar subunits is the optimal octupolar order and results in coherent second harmonic emission from each individual building-blocks (eq 3).⁴⁴ These supramolecular order was first illustrated by crystal engineering of functionalized triazines, but no clear NLO evidence was given.^{15a} To the best of our knowledge the present study is the

first example of supramolecular octupolar self-ordering within a dendritic architecture.⁴⁵

Conclusions

The present results show that coordination chemistry can be a useful tool for the design of molecular materials for nonlinear optics by combining bipyridyl ligands with ruthenium(II). The ability to substitute the pyridine rings with functional groups offers the possibility of incorporating octupolar NLO-phores into polymers. Thus, thermally stable polyimides featuring octupolar ruthenium trisbipyridyl complexes can be readily obtained by a polycondensation reaction. The controlled coordination strategy of bipyridines to Ru(II) has also been successfully used to build supramolecules such as the first metallogendrimer made of seven metallo-octupoles. These polymetallic species exhibit very intense absorption bands in the visible and long-lived luminescence which make them good candidates as components of model systems for photochemical and photoelectrochemical conversion of solar energy. The quadratic NLO-susceptibilities β of these macromolecules have been characterized by harmonic light scattering at 1.91 μm in order to rule out any two-photon fluorescence contribution to the harmonic signal. A comparison with the fully disordered NLO-polyimide provides clear evidence of a quasi-optimized octupolar ordering in the metallogendrimer. The next challenge is the macroscopic (bulk) noncentrosymmetric organization of these chromophores. Because electric-field poling is not applicable due to the absence of permanent dipole moment, optical poling has to be explored to tackle this problem.⁴⁶ The construction and control of nanosized objects with the goal of miniaturizing photonic devices is another major challenge. The results described in this paper are very promising and open new perspectives toward nanoscale photonic applications.

Experimental Section

Polyimide Ligand 5a. To a solution of **4a** (500 mg, 0.94 mmol) in 1-methyl-2-pyrrolidinone (NMP, 6 mL) was added dropwise a NMP solution (4 mL) of 6FDA (416 mg, 0.94 mmol) at 0 °C. The mixture was then stirred for 2 days at room temperature. After further addition of pyridine (1.25 mL, 34 mmol) and acetic anhydride (3.25 mL, 34 mmol), the solution was heated overnight at 60 °C. The solution was then cooled to room temperature and added dropwise in diethyl ether (200 mL) under vigorous stirring. The resulting precipitate was filtered off and recrystallized twice from dichloromethane (10 mL)-diethyl ether (200 mL). After filtration, the resulting yellow solid was dried under vacuum (690 mg, 82%). ¹H NMR (200.13 MHz, CD₂Cl₂) δ : 8.51 (m br, 2H, H₆); 8.45 (s br, 2H, H₃); 7.78 (m, 2H, H_{6FDA}); 7.75 (m, 4H, H_{6FDA}); 7.40–7.20 (m, 8H, H_{5,8,10}); 6.87 (d br, $J = 16.2$ Hz, 2H, H₇); 6.76 (d br, $J = 8.8$ Hz, 4H, H₁₁); 3.86 (m br, 4H, H₁₄); 3.58 (m br, 4H, H₁₃); 3.40 (m br, 4H, H_{13'}); 1.16 (m br, 6H, H_{14'}). ¹⁹F NMR (CD₂Cl₂) δ : -63.9 (s); IR (KBr) ν (cm⁻¹): 1778, 1718, 744; UV-visible (CH₂Cl₂): $\lambda_{\text{max}} = 388$ nm; emission (CH₂Cl₂): $\lambda_{\text{em}} = 466$ nm; TGA: $T_{\text{d5}} = 374$ °C; DSC analysis: $T_g = 210$ °C; elemental analysis calcd (%) for [C₅₃H₄₂N₆O₄F₆·1 CH₂Cl₂]_n: C 63.22, H 4.32, N: 8.19; found: C 62.91, H 4.36, N 8.05.

(43) Latterini, L.; Pourtois, G.; Moucheron, C.; Lazzaroni, R.; Brédas, J.-L.; Kirsch-De Mesmaeker, A.; De Schryver, F. C. *Chem. Eur. J.* **2000**, *6*, 1331–1335.

(44) Zyss, J. "Hypercubic octupolar molecular crystals for quadratic nonlinear optics", *Conference on Lasers and Electrooptics (CLEO) 2000*, paper CM15, p 47.

(45) Examples of macromolecular architectures with octupolar symmetry, such as molecularly bridged gold nanoparticles (Novak, J. P.; Brousseau, L. C.; Vance, F. W.; Johnson, R. C.; Lemon, B. I.; Hupp, J. P.; Feldheim, D. L. *J. Am. Chem. Soc.* **2000**, *122*, 12 029–12 030) and Bacteriorhodopsin trimers in purple membrane suspensions (Hendricks, E.; Vinckier, A.; Clays, K.; Persoons, A. *J. Phys. Chem.* **1996**, *100*, 19 672–19 680) have recently been reported. However these macromolecules do not feature octupolar subunits.

(46) Piron, R.; Toussaere, E.; Josse, D.; Brasselet, S.; Zyss, J. *Synth. Met.* **2000**, *115*, 109–119.

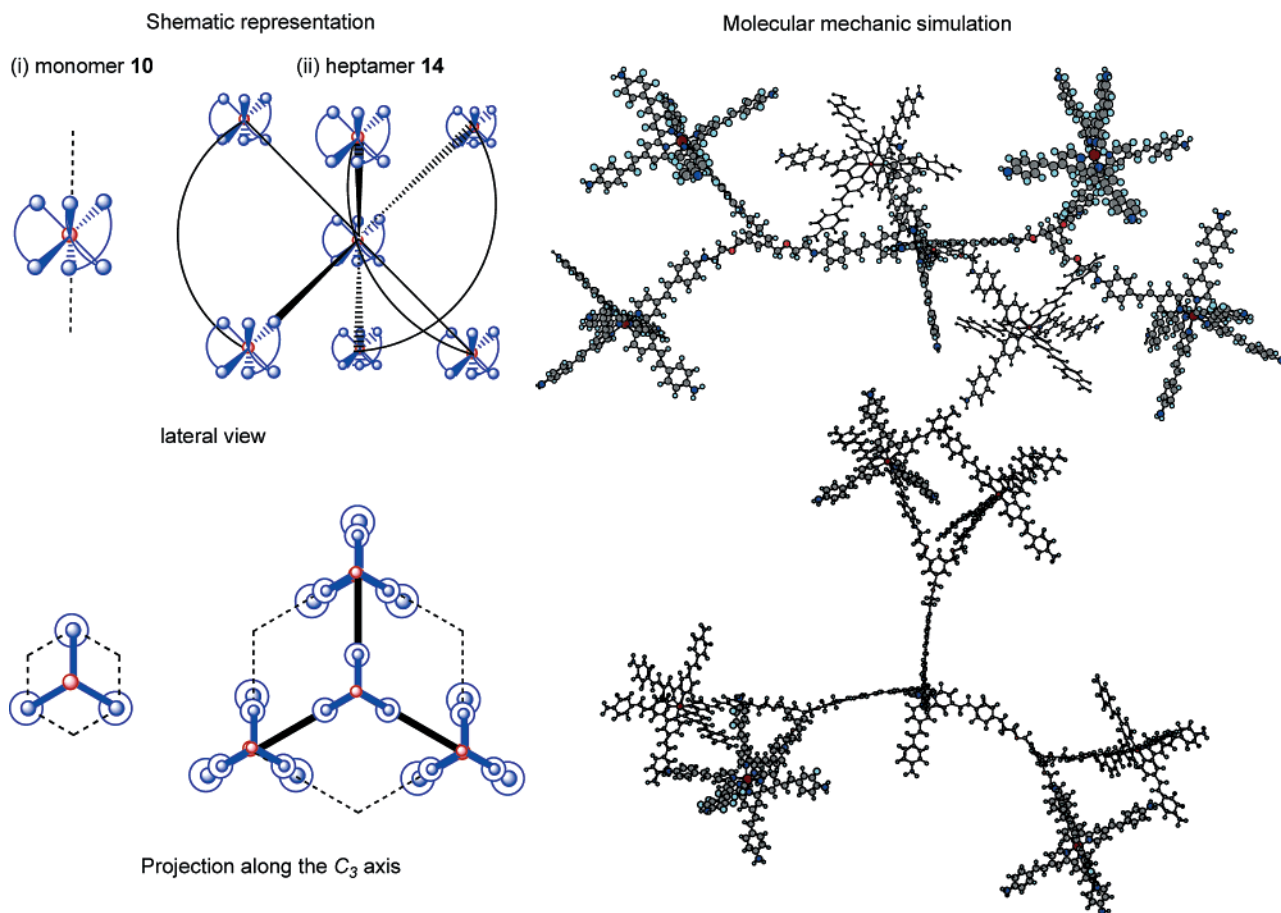


Figure 11. Molecular mechanics representation of one possible isomer of heptamer 14.

Polyimide Ligand 5b. Following the previous procedure, polymer **5b** was isolated as a yellow-orange powder (405 mg, 75%) from **4b** (350 mg, 0.54 mmol). ^1H NMR (200.13 MHz, CD_2Cl_2) δ : 8.53 (d br, $J = 5$ Hz, 2H, H_6); 8.46 (s br, 2H, H_3); 7.85 (m, 2H, $\text{H}_{6\text{FDA}}$); 7.77 (m, 4H, $\text{H}_{6\text{FDA}}$); 7.40–7.29 (m, 8H, $\text{H}_{5,8,10}$); 6.86 (d br, $J = 16.2$ Hz, 2H, H_7); 6.61 (d, $J = 8.9$ Hz, 4H, H_{11}); 3.69 (m br, 4H, H_{16}); 3.31 (m br, 8H, $\text{H}_{13,13'}$); 1.78–1.42 (m, 12H, $\text{H}_{14,14',15}$); 1.40–1.18 (m, 4H, $\text{H}_{15'}$); 0.91 (t br, $J = 7$ Hz, 6H, $\text{H}_{16'}$); RMN ^{19}F (CD_2Cl_2) δ : –63.9 (s); IR (KBr) ν (cm^{-1}): 1777, 1718, 743; UV–visible (CH_2Cl_2): $\lambda_{\text{max}} = 401$ nm; emission (CH_2Cl_2): $\lambda_{\text{em}} = 472$ nm; TGA: $T_{\text{d}5} = 398$ °C; DSC analysis: $T_g = 165$ °C; elemental analysis calcd (%) for $[\text{C}_{57}\text{H}_{50}\text{N}_6\text{O}_4\text{F}_6 \cdot 1.5 \text{CH}_2\text{Cl}_2]_n$: C 62.49, H 4.75, N: 7.47; found: C 62.44, H 5.31, N 6.78.

Polyimide Complex 7a. In a Schlenk flask, a DMF (12 mL) solution of **4b** (400 mg, 0.42 mmol) and **6a** (500 mg, 0.42 mmol) was heated under reflux for 6h. The dark-red solution was cooled to room temperature and an aqueous solution of NH_4PF_6 (277 mg, 1.7 mmol in 150 mL of water) was added. After 30 min of stirring, the dark-red precipitate was filtered off and washed successively with water (3×15 mL) and diethyl ether (3×15 mL). After recrystallization from dichloromethane-pentane, filtration and evaporation of the solvents, **7a** was recovered as a dark-red powder (922 mg, 93%). ^1H NMR (200.13 MHz, CD_2Cl_2) δ : 8.4 (m br, 6H, H_3); 7.85 (m br, 2H, $\text{H}_{6\text{FDA}}$); 7.74 (m br, 4H, $\text{H}_{6\text{FDA}}$); 7.50–7.20 (m, 30H, $\text{H}_{5,6,8,10}$); 6.90 (d, br, $J = 16$ Hz, 6H, H_7); 6.80–6.50 (m br, 12H, H_{11}); 3.90 (m br, 4H, H_{14}); 3.60 (m br, 4H, H_{13}); 3.40 (m br, 4H, $\text{H}_{13'}$); 1.16 (m, 30H, $\text{H}_{14'}$); ^{19}F NMR (CD_2Cl_2) δ : –63.9 (s); ^{31}P NMR (CD_2Cl_2) δ : –143 (hept, $J_{\text{P-F}} = 711$ Hz); IR (KBr) ν (cm^{-1}): 1777, 1718, 744; UV–visible (CH_2Cl_2): $\lambda_{\text{max}} = 441$ –509 nm; emission (CH_2Cl_2): $\lambda_{\text{em}} = 720$ nm; TGA: $T_{\text{d}5} = 350$ °C.

Polyimide Complex 7b. In a Schlenk flask, a DMF (7 mL) solution of **5b** (200 mg, 0.19 mmol) and **6b** (266 mg, 0.19 mmol) was heated

under reflux for 6h. The dark-red solution was cooled to room temperature and $[\text{HNBu}_3][\text{TRISPHAT}]$ (362 mg, 0.76 mmol) was added. After 30 min of stirring, a dark-red precipitate was obtained by addition of water (120 mL). The product was filtered off and washed successively with water (3×15 mL) and diethyl ether (3×15 mL). After recrystallization from dichloromethane-diethyl ether and filtration, **7b** was recovered as a dark-red powder (536 mg, 92%). ^1H NMR (200.13 MHz, CD_2Cl_2) δ : 8.44 (s br, 6H, H_3); 8.02 (m br, 6H, H_6); 7.90–7.72 (m, 6H, $\text{H}_{6\text{FDA}}$); 7.42–7.10 (m, 24H, $\text{H}_{5,8,10}$); 6.6 (m br, 18H, $\text{H}_{7,11}$); 3.73 (m br, 4H, H_{16}); 3.37 (m br, 8H, $\text{H}_{13,13'}$); 1.78–1.42 (m, 12H, $\text{H}_{14,14',15}$); 1.40–1.18 (m, 4H, $\text{H}_{15'}$); 0.91 (t br, $J = 7$ Hz, 6H, $\text{H}_{16'}$); ^{19}F NMR (CD_2Cl_2) δ : –63.9 (s); ^{31}P NMR (CD_2Cl_2) δ : –80.5 (s); IR (KBr) ν (cm^{-1}): 1777, 1718, 743; UV–visible (CH_2Cl_2): $\lambda_{\text{max}} = 445$ –513 nm; emission (CH_2Cl_2): $\lambda_{\text{em}} = 720$ nm; TGA: $T_{\text{d}5} = 358$ °C; elemental analysis calcd (%) for $[\text{C}_{169}\text{H}_{142}\text{N}_{14}\text{O}_{12}\text{Cl}_{24}\text{F}_6\text{P}_2\text{Ru} \cdot 2\text{H}_2\text{O}]_n$: C 54.49, H: 3.95, N: 5.26; found: C 54.83, H 4.77, N 4.92.

Dipod 8. In a Schlenk flask, bipyridine **2c** (156 mg, 0.3 mmol) was dissolved in dimethylformamide (6 mL). The yellow solution turned green during the slow addition of NaH (15 mg, 0.6 mmol). After stirring 1 h at 50 °C, a DMF solution (4 mL) of α, α' -dibromo-*p*-xylene (40 mg, 0.15 mmol) was added dropwise by mean of a syringe; the resulting brown mixture was stirred 2 days at 50 °C. After cooling at room temperature, the solution was added dropwise in water (250 mL) resulting in the formation of a yellow precipitate. The solid was filtered off and washed with water (3×50 mL) and diethyl ether (3×30 mL), dissolved in dichloromethane (30 mL) and dried over MgSO_4 . After filtration and evaporation of the solvent under vacuum, a yellow microcrystalline powder was recovered (161 mg, 94% yield). ^1H RMN (500.13 MHz, CD_2Cl_2) δ ppm: 8.52 (d, $J = 5$ Hz, 4H, $\text{H}_{6,6'}$), 8.46 (s, 4H, $\text{H}_{3,3'}$), 7.35 (s, 4H, H_{17}), 7.41–7.22 (m, 16H, $\text{H}_{10,10',8,8',5,5'}$), 6.87–6.86 (2d, $J = 16$ Hz, 4H, $\text{H}_{7,7'}$), 6.64–6.63 (2d, 8H, $\text{H}_{11,11'}$), 4.48 (s, 4H, H_{15}), 3.61 (t, $J = 6$ Hz, 4H, H_{14}), 3.52 (t, $J = 6$ Hz, 4H, H_{13}), 3.41

(q, $J = 7$ Hz, 4H, $H_{13''}$), 3.36 (q, $J = 7$ Hz, 8H, $H_{13'}$), 1.13 (t, $J = 7$ Hz, 12H, $H_{14'}$), 1.12 (t, $J = 7$ Hz, 6H, $H_{14''}$); ^{13}C RMN (125.33 MHz, CD_2Cl_2) δ ppm: 156.85 ($\text{C}_{2,2'}$), 149.69 ($\text{C}_{6,6'}$), 148.76–148.68 ($\text{C}_{12,12'}$), 146.99–146.92 ($\text{C}_{4,4'}$), 138.25 (C_{16}), 133.79–133.68 ($\text{C}_{8,8'}$), 128.96–128.88 ($\text{C}_{10,10'}$), 127.96 (C_{17}), 124.12–123.68 ($\text{C}_{9,9'}$), 121.30–120.99 ($\text{C}_{7,7'}$), 120.61 ($\text{C}_{5,5'}$), 117.86 ($\text{C}_{3,3'}$), 112.06–111.87 ($\text{C}_{11,11'}$), 73.39 (C_{15}), 68.41 (C_{14}), 50.47 (C_{13}), 45.84 ($\text{C}_{13''}$), 44.78 ($\text{C}_{13'}$), 12.80 ($\text{C}_{14'}$), 12.36 ($\text{C}_{14''}$); UV–visible (CH_2Cl_2): $\lambda_{\text{max}} = 395$ nm; $\epsilon_{\text{max}} = 90\,000$ $\text{l}\cdot\text{mol}^{-1}\cdot\text{cm}^{-1}$. TGA: $T_{\text{d}5} = 366$ °C; elemental analysis calcd (%) for $\text{C}_7\text{H}_8\text{N}_8\text{O}_2\cdot\text{H}_2\text{O}$: C 78.86, H 7.31, N 9.68; found: C 78.44, H 7.12, N 9.65; HRMS (FAB+) calcd for $\text{C}_7\text{H}_8\text{N}_8\text{O}_2$: 1139.6639, found: 1139.6640 $\{\text{M}+\text{H}\}^+$.

Tripod 9. In a Schlenk flask, bipyridine **2c** (750 mg, 1.45 mmol) was dissolved in DMF (15 mL). The yellow solution turned green during the slow addition of NaH (70 mg, 2.9 mmol). After stirring 1 h at 50 °C, a DMF solution (4 mL) of tris-1,3,5-bromomethyl-2,4,6-mesitylene (193 mg, 0.48 mmol) was added dropwise by means of a syringe; the resulting brown mixture was stirred 2 days at 50 °C. After cooling to room temperature, the solution was added dropwise in water (250 mL) resulting in the formation of a yellow precipitate. The solid was filtered off and washed with water (3×50 mL) and diethyl ether (3×30 mL), dissolved in dichloromethane (50 mL) and dried over MgSO_4 . After filtration and evaporation of the solvent under vacuum, a yellow microcrystalline powder was recovered (800 mg, 96% yield). ^1H NMR (500.13 MHz, CD_2Cl_2): $\delta = 8.53$ – 8.51 (d, $J = 5$ Hz, 6H, H_6 , H_6'), 8.46 (s, 6H, H_3 , H_3'), 7.4–7.2 (m, 24H, H_{10} , $H_{10'}$, H_8 , H_8' , H_5 , H_5'), 6.86–6.87–6.88 (d, $J = 16$ Hz, 6H, H_7 , H_7'), 6.64 (m, 12H, H_{11} , $H_{11'}$), 4.53 (s, 6H, H_{15}), 3.67 (t, $J = 5.8$ Hz, 6H, H_{14}), 3.51 (t, $J = 5.8$ Hz, 6H, H_{13}), 3.40 (q, $J = 7$ Hz, 6H, $H_{13''}$), 3.36 (q, $J = 7$ Hz, 6H, $H_{13'}$), 2.36 (s, 9H, H_{18}), 1.15 (t, $J = 7$ Hz, 18H, $H_{14'}$), 1.11 (t, $J = 7$ Hz, 9H, $H_{14''}$); ^{13}C NMR (125.33 MHz, CD_2Cl_2): $\delta = 156.81$ (C_2 , C_2'), 149.67 (C_6 , C_6'), 148.73–148.67 (C_{12} , $\text{C}_{12'}$), 146.99–146.90 (C_4 , C_4'), 138.40 (C_{16}), 133.78–133.68 (C_8 , C_8'), 133.17 (C_{17}), 128.95–128.92 (C_{10} , $\text{C}_{10'}$), 124.08–123.68 (C_9 , C_9'), 121.28–120.97 (C_7 , C_7'), 120.60 (C_5), 117.86 (C_3), 112.02–111.87 (C_{11} , $\text{C}_{11'}$), 68.62 (C_{15}), 68.38 (C_{14}), 50.59 (C_{13}), 45.88 ($\text{C}_{13''}$), 44.78 ($\text{C}_{13'}$), 15.94 (C_{18}), 12.80 ($\text{C}_{14'}$), 12.38 ($\text{C}_{14''}$); UV–visible (CH_2Cl_2): $\lambda_{\text{max}} = 396$ nm (130000); TGA: $T_{\text{d}5} = 348$ °C, $T_{\text{d}10} = 370$ °C; elemental analysis calcd (%) for $\text{C}_{114}\text{H}_{126}\text{N}_{12}\text{O}_3\cdot 2\text{H}_2\text{O}$: C: 78.32, H: 7.49, N: 9.61; found: C 78.14, H 7.20, N 9.51; HRMS (FAB+) calcd for $\text{C}_{114}\text{H}_{127}\text{N}_{12}\text{O}_3$: 1712.0154; found 1712.0256 $\{\text{M}+\text{H}\}^+$.

[(DEASbipy₂Ru)₂dipod][TRISPHAT]₄ or Dimer 11. In a Schlenk flask, ligand **8** (50 mg, 4.4×10^{-5} mol) and **6a** (103 mg, 8.8×10^{-5} mol) were dissolved in DMF (5 mL) and stirred during 5 h under reflux. After cooling to room temperature, [TRISPHAT][HNBu₃] (170 mg, 0.18 mmol) was added. After stirring 30 min at room temperature a dark red solid was precipitated by addition of water (150 mL). The complex was filtered off, washed with water (3×50 mL) and diethyl ether (3×30 mL), dissolved in dichloromethane (25 mL) and dried over MgSO_4 . After recrystallization from a mixture of CH_2Cl_2 –pentane, the solvents were removed under vacuum and a dark red microcrystalline powder was recovered (255 mg, 90% yield).

All diethylaminostyryl bipyridyl fragments have the same chemical shifts (^1H and ^{13}C). The only difference appears in the ethyl fragment of N– CH_2CH_2 –O linked to the phenyl core. ^1H RMN (500.13 MHz, CD_2Cl_2) δ ppm: 8.35 (s, 12H, $H_{3,3'}$), 8.01 (d, $J = 5$ Hz, 12H, $H_{6,6'}$), 7.4–7.2 (m, 28H, $H_{10,10'}$, $H_{8,8'}$, $H_{5,5'}$), 6.7–6.5 (m, 18H, $H_{11,11'}$, $H_{7,7'}$), 4.46 (s, 4H, H_{15}), 3.59 (s, 4H, H_{14}), 3.51 (s, 4H, H_{13}), 3.36 (m, 40H, $H_{13'}$), 3.17 (s, 4H, $H_{13''}$), 1.15 (m, 66H, $H_{14',14''}$). ^{13}C RMN (125.33 MHz, CD_2Cl_2) δ ppm: 157.34 ($\text{C}_{2,2'}$), 151.37 ($\text{C}_{6,6'}$), 149.44 ($\text{C}_{12,12'}$), 147.55 ($\text{C}_{4,4'}$), 138.18 (C_{16}), 136.75 ($\text{C}_{8,8'}$), 127.89 (C_{17}), 129.81 ($\text{C}_{10,10'}$), 122.90 ($\text{C}_{9,9'}$), 122.67 ($\text{C}_{5,5'}$), 120.05 ($\text{C}_{3,3'}$), 117.72 ($\text{C}_{7,7'}$), 111.79 ($\text{C}_{11,11'}$), 73.41 (C_{15}), 68.42 (C_{14}), 50.49 (C_{13}), 45.81 ($\text{C}_{13''}$), 44.86 ($\text{C}_{13'}$), 12.84 ($\text{C}_{14'}$), 12.41 ($\text{C}_{14''}$), TRISPHAT: 142.05 (d, $J = 7$ Hz), 123.06 (s), 114.38 (d, $J = 20$ Hz). ^{31}P RMN (81 MHz, CD_2Cl_2) δ ppm: –80.50 (s); UV–visible (CH_2Cl_2): $\lambda_{\text{max}} = 440$ nm; $\epsilon_{\text{max}} = 258\,000$ $\text{l}\cdot\text{mol}^{-1}\cdot\text{cm}^{-1}$, $\lambda_{\text{max}} =$

511 nm; $\epsilon_{\text{max}} = 239\,000$ $\text{l}\cdot\text{mol}^{-1}\cdot\text{cm}^{-1}$; TGA: $T_{\text{d}5} = 325$ °C; elemental analysis calcd (%) for $\text{C}_{284}\text{H}_{234}\text{N}_{24}\text{Cl}_{48}\text{O}_{26}\text{P}_4\text{Ru}_2\cdot 2\text{CH}_2\text{Cl}_2$: C 52.07, H 3.64, N: 5.10; found: C 52.21, H 3.57, N 5.26; LRMS (FAB+): only fragmentation peaks were observed: $\{[\text{DEASbipy}_2\text{Ru}(2)][\text{TRISPHAT}]\}^+ 2393.4$, $\{[\text{DEASbipy}_3\text{Ru}][\text{TRISPHAT}]\}^+ 2377.4$, $\{[\text{DEASbipy}_2\text{Ru}(2)]\}^{2+}$, 812.3, $\{[\text{DEASbipy}_3\text{Ru}]\}^{2+}$ 804.3.

[(DEASbipy₂Ru)₃tripod][TRISPHAT]₆ or Trimer 12. In a Schlenk flask, ligand **9** (100 mg, 5.84×10^{-5} mol) and complex **6a** (206 mg, 1.75×10^{-4} mol) were dissolved in DMF (10 mL) and stirred during 5 h under reflux. After cooling to room temperature, [TRISPHAT][HNBu₃] (335 mg, 0.35 mmol) was added. After stirring 30 min at room temperature, a dark red solid was precipitated by addition of water (200 mL). Complex **12** was filtered off, washed with water (3×50 mL) and diethyl ether (3×30 mL), dissolved in dichloromethane (50 mL) and dried over MgSO_4 . After recrystallization from a mixture of CH_2Cl_2 –pentane, the solvents were removed under vacuum and a dark red microcrystalline powder was recovered (520 mg, 92% yield).

All diethylaminostyryl bipyridyl fragments have the same chemical shifts (^1H and ^{13}C). The only difference appears in the ethyl fragment of N– CH_2CH_2 –O linked to the phenyl core. ^1H NMR (500.13 MHz CD_2Cl_2): $\delta = 8.46$ (s, 18H, H_3 , H_3'), 7.91 (d, $J = 5$ Hz, 18H, H_6 , H_6'), 7.4–7.3 (m, 54H, H_{10} , $H_{10'}$, H_8 , H_8'), 7.14 (d, $J = 5$ Hz, 18H, H_5 , H_5'), 6.68 (d, $J = 16$ Hz, 18H, H_7 , H_7'), 6.62 (d, $J = 9$ Hz, 36H, H_{11} , $H_{11'}$), 4.49 (s br, 6H, H_{15}), 3.64 (s br, 6H, H_{14}), 3.47 (s br, 6H, H_{13}), 3.36 (m, 60H, $H_{13'}$), 3.16 (s br, 6H, $H_{13''}$), 2.36 (br, 9H, H_{18}), 1.13 (m, 99H, $H_{14'}$, $H_{14''}$); ^{13}C NMR (125.33 MHz CD_2Cl_2): $\delta = 157.36$ (C_2 , C_2'), 151.11 (C_6 , C_6'), 149.39 (C_{12} , $\text{C}_{12'}$), 147.55 (C_4 , C_4'), 138.37 (C_{16}), 136.92 (C_8 , C_8'), 133.10 (C_{17}), 129.81 (C_{10} , $\text{C}_{10'}$), 122.95 (C_9 , C_9'), 122.72 (C_5), 120.21 (C_{13}), 117.78 (C_7 , C_7'), 110.93 (C_{11} , $\text{C}_{11'}$), 68.65 (C_{15}), 68.42 (C_{14}), 50.53 (C_{13}), 45.84 ($\text{C}_{13''}$), 44.83 ($\text{C}_{13'}$), 15.92 (C_{18}), 12.84 ($\text{C}_{14'}$), 12.40 ($\text{C}_{14''}$), TRISPHAT: 142.04 (d, $J = 7$ Hz), 123.05 (s), 114.38 (d, $J = 20$ Hz); ^{31}P NMR (81 MHz CD_2Cl_2): $\delta = -80.50$; UV–visible (CH_2Cl_2): $\lambda_{\text{max}} = 511$ nm (354000), $\lambda_{\text{max}} = 443$ nm (379000); TGA: $T_{\text{d}5} = 328$ °C, $T_{\text{d}10} = 352$ °C; elemental analysis calcd (%) for $\text{C}_{426}\text{H}_{354}\text{N}_{36}\text{Cl}_{72}\text{O}_{39}\text{P}_6\text{Ru}_3\cdot 3\text{CH}_2\text{Cl}_2$: C 52.06, H 3.67, N: 5.09; found: C 52.53, H 3.68, N 5.35; LRMS (FAB+): only fragmentation peaks were observed: $\{[\text{DEASbipy}_2\text{Ru}(2)][\text{TRISPHAT}]\}^+ 2393.4$, $\{[\text{DEASbipy}_3\text{Ru}][\text{TRISPHAT}]\}^+ 2377.4$, $\{[\text{DEASbipy}_2\text{Ru}(2)]\}^{2+}$ 812.3, $\{[\text{DEASbipy}_3\text{Ru}]\}^{2+}$ 804.3.

[Ru(tripod)₃][TRISPHAT]₂ 13. In a Schlenk flask, ligand **9** (250 mg, 1.46×10^{-4} mol) and $\text{RuCl}_2(\text{DMSO})_4$ (23.6 mg, 4.9×10^{-5} mol) were dissolved in DMF (6 mL) and the dark red solution was stirred during 5 h under reflux. After cooling to room temperature, [TRISPHAT][HNBu₃] (93 mg, 9.7×10^{-5} mol) was added. After stirring 30 min at room temperature a dark red solid was precipitated by addition of water (200 mL), then filtered off, washed with water (3×50 mL) and diethyl ether (3×30 mL), dissolved in dichloromethane (50 mL) and dried over MgSO_4 . After recrystallization from a CH_2Cl_2 –pentane mixture, a dark red microcrystalline powder was obtained (310 mg, 94% yield). As ^1H NMR signals are broad, their multiplicity are not given. However two types of bipyridyl protons and carbons can be distinguished: coordinated ligand noted *c* and free ligand noted *f*. C_{12c} , C_{7c} , and C_{4c} are not observed as they are masked by the TRISPHAT signals. ^1H NMR (500.13 MHz CD_2Cl_2): $\delta = 8.46$ (br, 12H, H_{6f}), 8.42 (br, 18H, H_{3f} , H_{3c}), 7.9 (br, 6H, H_{6c}), 7.4–7.2 (m, 72H, H_{10} , H_8 , H_{5f} , H_{5c}), 6.8 (d, 12H, H_{7f}), 6.60 (br, 42H, H_{7c} , H_{11}), 4.50 (s br, 18H, H_{15}), 3.63 (s br, 18H, H_{14}), 3.47 (s br, 18H, H_{13}), 3.32 (q br, 54H, H_{13} , $H_{13''}$), 2.33 (s br, 27H, H_{18}), 1.10 (t br, 81H, $H_{14'}$, $H_{14''}$); ^{13}C NMR (125.33 MHz CD_2Cl_2): $\delta = 157.27$ (C_{2c} , $\text{C}_{2'c}$), 156.70 (C_{6f} , $\text{C}_{6'f}$), 151.18 (C_{6c} , $\text{C}_{6'c}$), 149.64 (C_{6f} , $\text{C}_{6'f}$), 148.75–148.68 (C_{12f} , $\text{C}_{12'f}$), 147.47 (C_{4c} , $\text{C}_{4'c}$), 147.01–146.91 (C_{4f} , $\text{C}_{4'f}$), 138.41 (C_{16}), 136.84 (C_{8c} , $\text{C}_{8'c}$), 133.82 (C_{8f} , $\text{C}_{8'f}$), 133.02 (C_{17}), 129.76 (C_{10c} , $\text{C}_{10'c}$), 128.95 (C_{10f} , $\text{C}_{10'f}$), 123.59 (C_{9f} , $\text{C}_{9'f}$), 122.78 (C_{9c} , $\text{C}_{9'c}$), 122.47 (C_{5c}), 120.97 (C_{7f} , $\text{C}_{7'f}$), 120.64 (C_{5f}), 120.10 (C_{3c}), 117.86 (C_{3f}), 112.02–111.86 (C_{11f} , $\text{C}_{11'f}$), 68.61 (C_{14}), 68.36 (C_{15}), 50.59 (C_{13}), 45.87 ($\text{C}_{13''}$), 44.77 ($\text{C}_{13'}$), 15.94 (C_{18}), 12.81 ($\text{C}_{14'}$), 12.39 ($\text{C}_{14''}$). TRISPHAT: 142.06 (br), 123.03 (s), 114.36 (d, $J = 20$ Hz); ^{31}P

NMR (81 MHz CD_2Cl_2): $\delta = -80.5$; UV–visible (CH_2Cl_2): $\lambda_{\text{max}} = 518$ nm (97000), $\lambda_{\text{max}} = 400$ nm (306000); elemental analysis calcd (%) for $\text{C}_{378}\text{H}_{378}\text{N}_{36}\text{Cl}_{24}\text{O}_{21}\text{P}_2\text{Ru}_6\text{CH}_2\text{Cl}_2$: C 63.31, H 5.40, N 6.92; found: C 63.22, H 5.26, N 6.84.

[(DEASbipy₂Ru)₆(tripod)₃Ru][TRISPHAT]₁₄ or Heptamer 14. In a Schlenk flask, $[\text{Ru}(\text{tripod})_3][\text{TRISPHAT}]_2$ **13** (150 mg, 2.2×10^{-5} mol) and complex **6a** (156 mg, 0.13 mmol) were dissolved in DMF (6 mL) and stirred during 6 h under reflux. The solution turned from green-brown to deep red. After cooling to room temperature, $[\text{TRISPHAT}][\text{HNBu}_3]$ (253 mg, 0.26 mmol) was added. After stirring 1 h. at room temperature, a dark red solid was precipitated by addition of water (200 mL). The resulting complex was filtered off, washed with water (3×50 mL) and diethyl ether (3×30 mL), dissolved in dichloromethane (50 mL) and dried over MgSO_4 . After recrystallization from a CH_2Cl_2 –pentane mixture, the solvents were removed under vacuum and a dark red microcrystalline powder was obtained (450 mg, 91% yield). As ^1H NMR signals are broad, their multiplicity are not given. ^1H NMR (500.13 MHz CD_2Cl_2 5.28): $\delta = 8.3$ (br, 42H, $H_3 H_{3'}$), 8.0 (br, 42H, $H_6 H_{6'}$), 7.4–7.0 (b, 168H, $H_{10} H_{10'}$ $H_8 H_{8'}$ $H_5 H_{5'}$), 6.6 (br, 126H, $H_7 H_{7'}$ $H_{11} H_{11'}$), 4.5 (s br, 18H, H_{15}), 3.6–3.0 (m br, 182H, $H_{14} H_{13} H_{13'}$ $H_{13''}$), 2.3 (br, 27H, H_{18}), 1.1 (m br, 231H, $H_{14'} H_{14''}$). C_9 and $C_{9'}$ are not visible, they are fused in one of the TRISPHAT signals; ^{13}C NMR (125.33 MHz CD_2Cl_2): $\delta = 157.30$ ($C_2 C_{2'}$), 151.36 ($C_6 C_{6'}$), 149.44

($C_{12} C_{12'}$), 147.46 ($C_4 C_{4'}$), 138.36 (C_{16}), 136.61 ($C_8 C_{8'}$), 133.08 (C_{17}), 129.81 ($C_{10} C_{10'}$), ($C_9 C_{9'}$), 122.63 (C_5), 120.13 (C_3), 117.69 ($C_7 C_{7'}$), 111.76 ($C_{11} C_{11'}$), 68.67 (C_{15}), 68.67 (C_{14}), 50.59 (C_{13}), 45.82 ($C_{13''}$), 44.85 ($C_{13'}$), 15.94 (C_{18}), 12.84 ($C_{14'}$), 12.41 ($C_{14''}$), TRISPHAT: 142.05 (d, $J = 7$ Hz), 123.04 (s), 114.39 (d, $J = 20$ Hz); ^{31}P NMR (81 MHz CD_2Cl_2): $\delta = -80.5$; UV–visible (CH_2Cl_2): $\lambda_{\text{max}} = 444$ nm (693000), $\lambda_{\text{max}} = 506$ nm (648000); TGA: $T_{d5} = 321$ °C, $T_{d10} = 355$ °C; elemental analysis calcd (%) for $\text{C}_{1002}\text{H}_{834}\text{N}_{84}\text{Cl}_{168}\text{O}_{93}\text{P}_{14}\text{Ru}_{7.14}\text{CH}_2\text{Cl}_2$: C 51.22, H 3.65, N 4.94; found: C 50.71, H 3.58, N 5.34.

Acknowledgment. This research was supported by the *Ministère de la recherche* (FNS-Program nanostructure), the CNRS, the *Région Bretagne* (PRIR A2CA16) and the CNET (France-Telecom) for a grant to T.L.B.

Supporting Information Available: General considerations on spectroscopic, thermal analysis, photophysical and NLO measurements and theoretical calculations. Synthetic procedures and characterization data of bipyridines **3a**, **3b**, **4a**, **4b**, and ruthenium complex **6b**. This material is available free of charge via the Internet at <http://pubs.acs.org>.

JA030296J